Zoological Journal of the Linnean Society, 2017, **180**, 243–267. With 11 figures.

Unmasking *Aurelia* species in the Mediterranean Sea: an integrative morphometric and molecular approach

SIMONETTA SCORRANO[1,2]*, GIORGIO AGLIERI[1,2], FERDINANDO BOERO[1,2,3], MICHAEL N. DAWSON[4] and STEFANO PIRAINO[1,2]*†

[1]*CoNISMa, Consorzio Nazionale Interuniversitario per le Scienze del Mare, Roma, Italy*
[2]*Dipartimento di Scienze e Tecnologie Biologiche ed Ambientali (DiSTeBA), Università del Salento, Lecce, Italy*
[3]*Consiglio Nazionale delle Ricerche, Istituto di Scienze Marine (ISMAR-CNR), Genova, Italy*
[4]*School of Natural Sciences, University of California, Merced CA, 95343, USA*

Received 3 February 2016; revised 1 August 2016; accepted for publication 13 August 2016

Molecular analyses have led to an increased knowledge of the number and distribution of morphologically cryptic species in the world's oceans and, concomitantly, to the identification of non-indigenous species (NIS). Traditional taxonomy and accurate delimitation of species' life histories and autecology lag far behind, however, even for the most widely distributed taxa, such as the moon jellyfish *Aurelia* (Cnidaria, Scyphozoa) species complex. Here we analysed mitochondrial cytochrome *c* oxidase subunit I (*COI*) and nuclear 28S ribosomal RNA (*28S*) gene sequences to assign polyps, ephyrae, and medusae collected in the Mediterranean Sea to different phylogenetic species. We find evidence for three *Aurelia* species, none of which are referable to the type species of the genus, *Aurelia aurita* (Linnaeus, 1758), and describe the anatomical, morphometric, and developmental variation within and between them. We identify *Aurelia coerulea* von Lendenfeld, 1884 and *Aurelia solida* Browne, 1905 as established non-indigenous species in the Mediterranean Sea. We describe ***Aurelia relicta* sp. nov.**, an endemic species currently unique to a population in the marine lake of Mljet (Croatia). These results demonstrate the usefulness of integrative approaches in resolving taxonomic uncertainty surrounding cryptic species complexes, identifying patterns of marine biodiversity, and recognizing non-indigenous species in marine ecosystems.

doi: 10.1111/zoj.12494

ADDITIONAL KEYWORDS: cryptic species – ephyra – integrative taxonomy – medusa – moon jellyfish – non-indigenous species – phylogeography – polyp – Scyphozoa.

INTRODUCTION

Species identification is a crucial initial step for exploring biodiversity, including understanding functional interactions among the components of any ecosystem. Species concepts and methods have been elaborated to clarify, formalize, and increase the accuracy of species identifications, including the recent integration of morphological data with molecular, geographical, ecological, reproductive, and behavioural data (DeSalle, Egan & Siddal, 2005). Looking for congruence among multiple classes of characters, 'integrative taxonomy' is often applied to distinguish or define cryptic species (Padial *et al.*, 2010).

Nevertheless, when knowledge of the taxonomy and phylogeography of a group is limited, selecting characters that reliably distinguish subtaxa may become a circular process if independent validation is lacking. To address this issue, approaches relying on molecular phylogenetics (De Queiroz & Gauthier, 1992; Mishler & Theriot, 2000) or on 'bar-coding' mitochondrial DNA (Hebert *et al.*, 2003) have gained

*Corresponding authors. E-mails: simonetta.scorrano@unisalento.it and stefano.piraino@unisalento.it
†Senior author.
[Version of Record, published online 21 October 2016; http://zoobank.org/urn:lsid:zoobank.org:pub:A7E14A6A-CBE6-4786-865D-54EB746D4182]

prominence. Specimens may be assigned to undescribed species, known species, or species complexes, providing a stimulus to reconsider the status of knowledge in poorly known taxa (e.g. Martin *et al.*, 1997; Piraino *et al.*, 2014). The resulting taxonomic revisions may then lead to the identification of previously unnoticed diagnostic characters (Gershwin & Collins, 2002; Morandini & Marques, 2010), and, at the same time, suggest new interpretations of functional traits and their ecological implications (Dawson & Hamner, 2009; Bayha & Dawson, 2010).

For example, the moon jellyfish *Aurelia* has been regarded for several decades as a taxon represented by just two valid species (Kramp, 1968; Russell, 1970): the putatively cosmopolitan *Aurelia aurita* (Linnaeus, 1758), with broad temperature and salinity tolerance (Kramp, 1961; Russell, 1970; Papathanassiou, Panayotidis & Anagnostaki, 1987; Arai, 1997), and the cold-water boreal *Aurelia limbata* (Brandt, 1835). A third morphospecies, *Aurelia labiata* Chamisso & Eysenhardt, 1821, native to the Pacific coast of North America, was again acknowledged at the turn of the century (Wrobel & Mills, 1998; Gershwin, 2001). More recently, over the course of 5 years 13 additional *Aurelia* molecular species (Dawson & Jacobs, 2001; Dawson & Martin, 2001; Schroth *et al.*, 2002; Dawson, 2003; Dawson, Gupta & England, 2005) have been recognized around the globe. This implies that rather than a few widely distributed species there are many regional, possibly locally adapted, species of *Aurelia* (Dawson & Martin, 2001).

Reports of nuisance gelatinous plankton blooms have increased worldwide over the past half century (Boero *et al.*, 2008; Brotz *et al.*, 2012), but there is some confusion about the species involved (Lucas & Dawson, 2014). To date, limited molecular analyses have indicated the occurrence of: (1) a potential Lessepsian non-indigenous species (NIS) *Aurelia* sp. 8, in the Northern Adriatic Sea (Dawson *et al.*, 2005; Ramšak, Stopar & Malej, 2012) and the Gulf of Lyon (Schroth *et al.*, 2002); (2) a cold-water relict, *Aurelia* sp. 5, in the Mljet Lake in Croatia (Dawson & Jacobs, 2001); and (3) a sporadic record of *Aurelia* sp. 1 from French Mediterranean coastal waters (Schroth *et al.*, 2002). Nevertheless, none of the molecular data for Mediterranean specimens were complemented by morphological analyses, preventing species identifications or comparisons with described species.

A better understanding of underlying mechanisms calls for novel explicit morphological keys (e.g. Straehler-Pohl & Jarms, 2010; Gambill & Jarms, 2014) and integrative approaches, combining morphological, ecological, and molecular data (Dawson, 2003; Dawson & Hamner, 2009; Lee *et al.*, 2013). The real benefits offered by DNA-based identification of species lie in the definition of sequences as standardized comparative characters to support and integrate the morphological data set. To reconcile molecular and traditional morphological identifications of species, it is necessary to measure the same suites of characters with the same methods in populations across a wide geographic range, preferably including type localities (Dawson, 2003).

The present study addressed the taxonomic uncertainty surrounding *Aurelia* species in the Mediterranean Sea. We highlight relevant differences and similarities of morphological characters in three life stages – polyp, ephyra, and medusa – of *Aurelia* spp., first delimited by analysis of the mitochondrial cytochrome *c* oxidase subunit I (*COI*) and the nuclear ribosomal large subunit rDNA (*28S*) gene sequences.

MATERIAL AND METHODS

Study localities and sample collection

Morphological analyses were carried out on three life stages of *Aurelia* spp. from four Mediterranean localities: the tourist marina of Empuriabrava, Spain (Balearic Sea), the Mljet Lakes, Croatia (Adriatic sea), the Gulf of Trieste (Northern Adriatic sea), and the Varano Lagoon, Italy (Central Adriatic sea; Fig. 1). Polyps were collected by SCUBA diving (Mljet) or obtained in the laboratory after metamorphosis of planulae collected from sampled female jellyfish. Ephyrae were collected in the laboratory from temperature-dependent or pharmacological induction of strobilation (Kuniyoshi *et al.*, 2012; Fuchs *et al.*, 2014). In the laboratory, polyps and ephyrae were reared in 0.45-μm filtered seawater at constant temperature and salinity (T = 14 °C, S = 37), and fed daily with *Artemia salina* (Linnaeus, 1758) nauplii. After the polyps and ephyrae fed on *Artemia salina* for 2 hours, the containers were cleaned with swabs; seawater and uneaten food were discarded and replaced with filtered seawater under the same conditions. Polyps and ephyrae were described the following day, with empty guts. Polyp cultures were maintained and monitored from October 2012 to July 2013. Adult medusae were collected by hand net in the field and preserved in buffered 4% formalin solution (v/v in seawater, pH 7.2) for morphometric analyses.

Additional *Aurelia* specimens (medusae) were sampled for genetic analyses across the Mediterranean Sea, the North-East Atlantic, and the North Sea. A total of 63 specimens was collected from eight Mediterranean localities: Varano Lagoon and Mljet Lakes (western and eastern Adriatic sea, $N = 9$ and 11, respectively), Gulf of Trieste (northern Adriatic

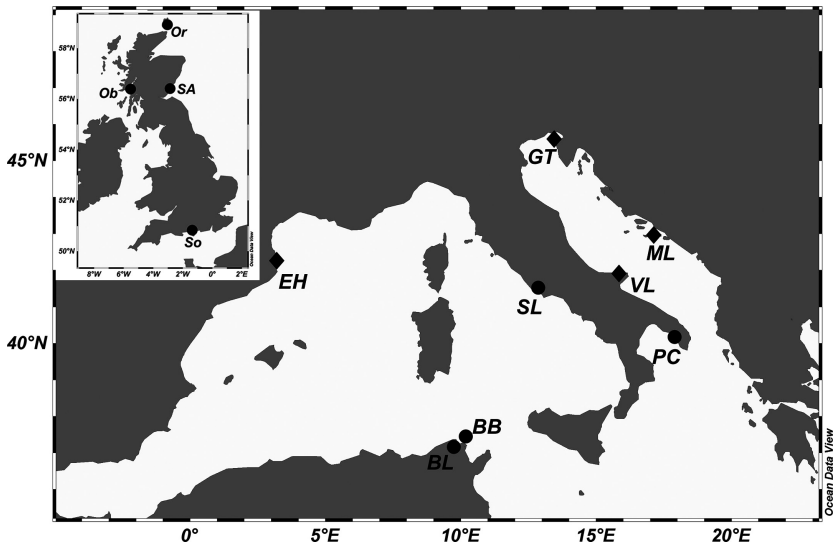

Figure 1. Locations of *Aurelia* spp. collected in the Mediterranean Sea and from northern European coasts: BB, Bizerte Bay (Tunisia); BL, Bizerte Lagoon (Tunisia); EH, Empuriabrava Harbour (Spain); GT, Gulf of Trieste (Italy); ML, Mljet lakes (Croatia); Ob, Oban (UK); Or, Orkney (UK); PC, Porto Cesareo (Italy); So, Southampton (UK); SA, St Andrews (UK); SL, Sabaudia Lake (Italy); VL, Varano Lagoon (Italy). Diamonds indicate locations for which both morphological and molecular analyses were performed; dots indicate locations where only genetic analyses were performed.

Sea, $N = 8$), Porto Cesareo (Ionian Sea, $N = 4$), Sabaudia Lake (Tyrrhenian Sea, $N = 1$), Empuriabrava Harbour (Balearic Sea, $N = 15$), Bizerte Bay and Bizerte Lagoon (southern Mediterranean Sea, $N = 3$ and 8, respectively); three localities in the North-East Atlantic (Southampton, $N = 1$; Oban, $N = 1$; Orkney, $N = 1$); and one from the North Sea (St Andrews, $N = 1$). Details on samples and their origins are provided in Figure 1 and Table S1. Samples were taken by hand net and a little piece (4–5 cm in diameter) of bell margin or oral arm was preserved in 95% ethanol at –20°C until DNA extraction. The tissues from all the specimens used for the genetic analyses are stored at the DNA and tissue bank of the Evolutionary Biology Lab, Dipartimento di Scienze e Tecnologie Biologiche ed Ambientali, Università del Salento, Lecce, Italy.

Molecular analyses

Total genomic DNA was extracted from the ethanol-preserved tissues, following a cetyltrimethylammonium bromide (CTAB) phenol chloroform-based protocol (Dawson, Raskoff & Jacobs, 1998; Dawson & Martin, 2001). Polymerase chain reactions (PCRs) were performed using an Eppendorf Mastercycler Gradient thermal cycler. Mitochondrial cytochrome *c* oxidase subunit I (*COI*) was amplified using the primers LCOjf (Dawson, 2005) and HCO2198 (Folmer *et al.*, 1994) with the PCR profile described elsewhere (Piraino *et al.*, 2014). The *28S* nuclear ribosomal large subunit rDNA was amplified using the primer pair Aa_L28S_21 and Aa_H28S_1078 (Bayha *et al.*, 2010), applying the reaction conditions suggested by the authors, except for the annealing temperature, which was increased to 53°C. The size and quality of the PCR products were examined on 1.5% agarose gels stained with GelRed™, and then purified with DE-001 GEL/PCR extraction and purification kit (Fisher Molecular Biology). The purified products were used as the template DNA for cycle sequencing reactions, performed by Macrogen (http://www.macrogen.com). Both DNA strands were sequenced. Each sequence was viewed with 4PEAKS (http://nucleobytes.com/index.php/4peaks) and paired strands were assembled using CAP3 (Huang & Madan, 1999), enabling the corroboration of forward and reverse reads. The identity of the sequences was confirmed using BLASTn to match them against the nucleotide collection (nr/nt) database of the National Center for Biotechnology Information (NCBI, http://www.ncbi.nlm.nih.gov). *COI* sequences were translated into amino acid sequences using the coelenterate mitochondrial code in MEGA 6.0 to confirm open reading frames.

The new data set included a total of 63 *COI* sequences of *Aurelia* spp. from all the considered sampling sites and 45 *28S* sequences from the same places, excluding Sabaudia Lake. The *COI* and *28S* sequences were used separately for within- and between-population genetic distance analyses and for single-locus phylogenetic analyses, and jointly for concatenated and coalescent-based phylogenetic analyses. For phylogenetic analyses aimed at evaluating the membership of the considered specimens to clearly

differentiated phylogenetic species, we added *COI* and *28S* sequences from GenBank for *A. aurita* (*N* = 4): *Aurelia* sp. 1 (*N* = 3), *Aurelia* sp. 2 (*N* = 1), *Aurelia* sp. 3 (*N* = 1), *Aurelia* sp. 4 (*N* = 1), *Aurelia* sp. 6 (*N* = 1), *Aurelia* sp. 8 (*N* = 2), *Aurelia* sp. 9 (*N* = 1), *Aurelia* sp. 10 (*N* = 1), and *Aurelia limbata* (*N* = 1). With the requirement of concatenated and coalescent-based analyses, only specimens with both *COI* and *28S* sequences were selected; for this reason, reference sequences for *A. aurita*, *Aurelia* sp. 5, *Aurelia* sp. 7, and *A. labiata* were not included in these analyses. In order to obtain a comprehensive picture of *Aurelia* phylogeography, however, we built an additional *COI* data set inclusive of all known species, including *A. aurita* (*N* = 4), *Aurelia* sp. 5 (*N* = 2), *Aurelia* sp. 7 (*N* = 1), and *A. labiata* (*N* = 2). The final data sets were composed of 57 specimens for the concatenated and coalescent-based analyses, and 82 specimens for the parallel single-gene *COI* analysis (for details, see Table S1). A *28S* sequences data set was also built to run a single locus analysis aimed at highlighting possible divergences between the mitochondrial and the nuclear gene trees. Sequences were aligned with CLUSTALX 2.0 (Thompson *et al.*, 1997) using default parameters and then visually checked, and, when necessary, trimmed to remove primer sequences with MacClade 4.08a (Maddison & Maddison, 2005).

The *COI* and *28S* pairwise genetic distances among samples were assessed with MEGA 6.0, separately for each marker, using the Kimura two-parameter (K2P) model of sequence evolution (Kimura, 1980) and estimating the variance by bootstrapping (1000 replicates). Sequences were grouped according to the sampling locality, and mean intragroup and intergroup distance matrices were generated. According to a recent study by L.E. Gómez Daglio & M. N. Dawson (unpublished data), the intraspecific genetic distances (K2P) in Discomedusae never exceed 6%, in agreement with an estimate for the maximum bar-coding gap in medusozoans of 5.7% previously proposed by Ortman *et al.* (2010). For this reason, in the present study, genetic distances higher than 6% in *COI* were interpreted as supportive of interspecific differences within *Aurelia* lineages.

COI and *28S* were concatenated with SEQUENCE MATRIX (Vaidya, Lohman & Meier, 2011). The best-fitting base substitution models and partition schemes were chosen for the alignments (*28S*, *COI*, and concatenated *28S–COI*) using the programs jModeltest 2.1.4 (Guindon & Gascuel, 2003; Darriba *et al.*, 2012) and PartitionFinder 1.1.1 (Lanfear *et al.*, 2012), and employing the Bayesian information criterion (BIC).

Species trees were reconstructed using the coalescent-based approach in *BEAST (Heled & Drummond, 2010), of the BEAST 1.8 package (Drummond *et al.*, 2012), applying three independent runs of 50 million generations each and sampling every 1000 steps. Each run employed the HKY+I base substitution model for the *28S* partition and the GTR+I model for *COI*, a Yule tree prior, and an uncorrelated lognormal relaxed clock. As *BEAST requires the *a priori* assignment of individuals to species, the results of the BLASTn searches and the MEGA genetic distance analyses on the data set were used to assign every individual to a given species. Convergence and stationarity of model parameters were checked with TRACER 1.6 and the runs were combined in LogCombiner 1.8 after a 20% burn-in. A maximum clade credibility tree with median ages was compiled with TreeAnnotator 1.8.0.

To compare *BEAST results with trees generated using the concatenated approach, additional maximum-likelihood analyses were performed in GARLI 2.1 (Zwickl, 2006) using the web service hosted at molecularevolution.org (Bazinet, Zwickl & Cummings, 2014). The analyses consisted of three replicates from a random starting tree topology and branch support estimates obtained by bootstrapping for 2000 iterations. The models of base substitution used were TpM3uf+I for *28S* and TIM+I for *COI*. The same parameters were also applied to perform two parallel single-locus analyses, using the *COI* alignment inclusive of the reference sequences for all known *Aurelia* species and the *28S* alignment.

The bootstrap support values for the GARLI trees were summarized with the SUMTREES 3.3.1 script implemented in DendroPy 3.8.0 (Sukumaran & Holder, 2010). All trees were drawn in FigTree 1.4.2 (http://tree.bio.ed.ac.uk./software/figtree).

Morphological and morphometrics analysis

For each population, 30 polyps, six ephyrae, and between seven and ten medusae were selected randomly for analysis of morphology and anatomy (Dawson, 2003; Straehler-Pohl & Jarms, 2010; Straehler-Pohl, Widmer & Morandini, 2011). The morphometric variables used in this study for each life-history stage are shown in Figure 2. The morphology of polyp and ephyra were measured using live animals mounted on a microscope depression slide. The development of the gastric system in ephyrae was studied from time 0 (days since strobilation of ephyrae) to week 4. Microphotographs were taken with a Nikon AW110 and Nikon Coolpix 990 digital camera on a Leica MZ 12 stereoscope. The measurements and incorporation of scale bars were performed with ImageJ (Abramoff, Magalhaes & Ram, 2004).

For the medusa stage, features of tissue colour and total wet mass (f14, f15, f16, f17, and f4; Dawson, 2003) were not considered to result from

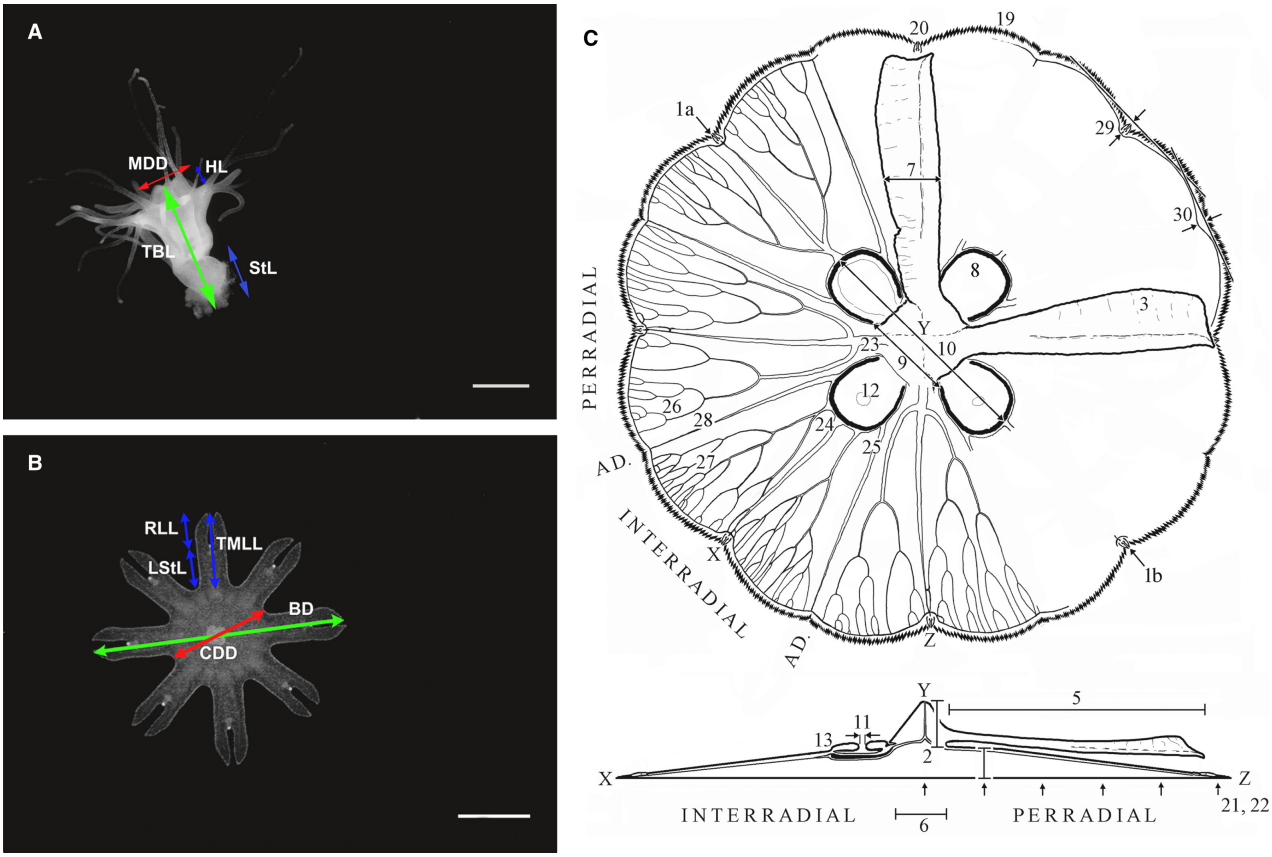

Figure 2. Morphometric measures analysed in three life stages of *Aurelia* spp. A, polyp stage: HL, hypostome length; MDD, mouth disc diameter; StL, stalk length; TBL, total body length. B, ephyra stage: BD, bell diameter; CDD, central disc diameter; LStL, lappet stem length; RLL, rhopalial lappet length; TMLL, total marginal lappet length. C, medusa stage: f1, bell diameter (mm from 1a to 1b); f2, manubrium depth (mm); f3, folding of the oral arm (0–2, half-point intervals); f5, oral arm length (mm); f6, manubrium width (mm); f7, oral arm width (mm); f8, gastric pouch shape; f9, proximal gastric diameter (PGD, mm); f10, distal gastric diameter (DGD, mm); f11, subgenital pore diameter (mm); f12, subgenital pore position (central, inside, overlapping, outside); f13, subgenital pore thickening (0–2, half-point intervals); f19, number of lobes; f20, number of rhopalia; f21, bell shape; f22, bell thickness; f23, perradial origins (qtr^{-1}); f24, interradial origins (qtr^{-1}); f25, adradial origins (qtr^{-1}); f26, perradial anastomoses (qtr^{-1}); f27, interradial anastomoses (qtr^{-1}); f28, adradial anastomoses (qtr^{-1}); f29, rhopaliar indent (mm); f30, non-rhopaliar indent (mm). Scale bars: A, B, 1 mm.

formaldehyde preservation. Medusae from Mljet were not reproductively mature, so the measures relative to sex and subgenital pore (f11, f12, and f13) were not considered in the overall comparison.

Abbreviations

Collection locations

BB, Bizerte Bay; BL, Bizerte Lagoon; EH, Empuriabrava Harbour; GT, Gulf of Trieste; ML, Mljet Lakes; Ob, Oban; Or, Orkney; PC, Porto Cesareo; S, Southampton; SA, St Andrews; SL, Sabaudia Lake; VL, Varano Lagoon.

Sample repositories

UNIPD, Collection of the Cnidaria at the Museum of Adriatic Zoology Giuseppe Olivi (Palazzo Grassi, Chioggia) of the University of Padova; UNIS_SCY, Collection of Scyphozoa of the Laboratory of Zoology and Marine Biology in the University of Salento (Lecce).

Data analyses

To explore potential effects of allometric growth, morphometric variables were regressed against total body length (TBL) in polyps, and against bell diameter (BD) in ephyrae and medusae. Features showing significant linear correlation at $\alpha = 0.05$ and with a power of ≥ 0.8 were considered isometric. Features that did not change with size were included in subsequent analyses without any transformations; isometric features were regressed and corrected according to the method described in Allisson *et al.* (1995),

then new variables were rescaled to BD. No features scaled allometrically with BD.

Statistical analyses were performed with PRIMER 6+ (Plymouth Marine Laboratory) using a significance threshold of 0.05 (Clarke & Warwick, 2001). A resemblance matrix based on Euclidean distance was calculated on normalized data in each life stage. All data were analysed using permutational multivariate analysis of variance (PERMANOVA), with 'population' as a fixed factor (Anderson, 2001). Subsequent pairwise tests of each feature of the polyp, ephyra and medusa stages led to the identification of characters that differed significantly among populations.

For all life stages, one-way similarity percentage analyses (SIMPER) were used to determine which characters contributed most to the dissimilarity between populations of *Aurelia* spp. Finally, a constrained canonical analyses of principal coordinates (CAP) tests the null hypothesis of no difference among the groups (populations) by first calculating a trace statistic (tr, $\text{trace}_{Q\_m'HQ\_m}$) and a P value based on permutations, and then finding the axes in the principal coordinate space that best discriminate among the hypothesized groups (Anderson & Willis, 2003).

RESULTS

Molecular analyses

Pairwise interpopulation K2P distances ranged between 0 and 22.3% (mean 11.3%) for the *COI* data set, and between 0 and 4.4% (mean 1.6%) for *28S*. The mean genetic distance within groups was 0.4% for *COI* and 0.3% for *28S*; the average between-groups difference was 14.2% for *COI* and 1.7% for *28S* (Table 1).

Two groups of samples showed very low inter-site mean K2P distances, far from the predefined interspecific limit of 6% in *COI*: (1) VL, SL, and EH, with between-group genetic distances of *COI* ≤ 0.7% and *28S* = 0.4%; and (2) BB, BL, GT, and PC, with between-group distances of *COI* ≤ 0.5% and *28S* ≤ 0.3%. Specimens from ML had mean within-population K2P distances of *COI* = 0.2% and *28S* = 0.9%, and mean distances for all other locations of *COI* = 19.8% and *28S* = 2.4%. Specimens from the UK showed within-group mean K2P distances of *COI* = 0.5% and *28S* = 0.1%, and mean distances for all other locations of *COI* = 20.8% and *28S* = 2.8%. In total, the pairwise comparisons indicate the differentiation of four distinct *Aurelia* species.

The maximum-likelihood (ML) analysis of the partitioned concatenated data set (Fig. 3) produced a phylogeny in general agreement with the coalescent species-tree analyses (Fig. 4). Although the coalescent and ML-partitioned approaches failed to resolve some weakly supported internal nodes, both clearly confirmed close genetic relationships within three clades: (1) *Aurelia* sp. 2 and *Aurelia* sp. 9 in the western South Atlantic Ocean; (2) *Aurelia* sp. 3, *Aurelia* sp. 4, and *Aurelia* sp. 6 in the tropical western Pacific; and (3) a subtropical and temperate western Pacific clade, including *A. limbata*, *Aurelia* sp. 1, and *Aurelia* sp. 10. No significant differences were highlighted in the ML analysis of the *COI* data set with reference sequences for all known *Aurelia* species. The tree showed the same topology as the coalescent and concatenated analyses, with *Aurelia* sp. 7 and *A. labiata* closely related to the Pacific *Aurelia* sp. 3, *Aurelia* sp. 4, and *Aurelia* sp. 6, and the reference sequences of *Aurelia* sp. 5 and *A. aurita* (both from the North Atlantic and Sea of Marmara) clustered with specimens from the Mljet lakes and the UK, respectively (Fig. S1). The single-locus analysis of *28S* (Fig. S2) corroborates the phylogeny generated by the *COI* analysis, even if the lower variability of the nuclear marker produced lower node support values and did not clearly separate some of the reference GenBank sequences. In particular, according to the *28S* gene tree, *Aurelia* sp. 3 and *Aurelia* sp. 4 appear to be closer to *Aurelia* sp. 5, whereas *Aurelia* sp. 6 appears to be closer to *Aurelia* sp. 1. Anyway, the substantial difference in length among the *28S* sequences available in GenBank (sequence length ranging from 102 to 207 nucleotides) might be responsible for the apparent incomplete phylogenetic differentiation among the aforementioned species.

All trees unequivocally confirmed that the specimens newly sampled in this study belong to four distinct clades supported by moderate to high statistical support values: (1) *Aurelia* sp. 1 from VL and SL, Italy, and EH, Spain; (2) *Aurelia* sp. 5 from ML, Croatia (3); *Aurelia* sp. 8 from BB and BL, Tunisia, and GT and PC, Italy; and (4) *A. aurita* from Ob, Or, So, and SA, UK.

Morphological and morphometric analyses of the Mediterranean *Aurelia* spp.

The selected morphological features exhibit a range of variations, with partial overlap across the three identified Mediterranean *Aurelia* clades (Table 2). Despite this, a PERMANOVA main test indicated highly significant differences for populations in terms of polyp morphometrics (Pseudo-F = 17.65, P < 0.01), ephyra (Pseudo-F = 4.60, P < 0.01), and medusae (Pseudo-F = 6.01, P < 0.01).

The PERMANOVA pairwise test showed that two characters – MDD/TBL and StL/TBL – differentiated the polyp stage of *Aurelia* sp. 5 from the polyp

Table 1. Mean sequence distances calculated using the Kimura two-parameter (K2P) model for *COI* and *28S*, within and between sampling localities and species

(A)

Area	Locality	Within-group mean genetic distances	
		COI	*28S*
Croatia: Adriatic Sea	ML	0.2 ± 0.1	0.9 ± 0.2
Italy: Adriatic Sea	GT	0.4 ± 0.2	0.0 ± 0.0
	VL	0.6 ± 0.2	0.1 ± 0.1
Italy: Ionian Sea	PC	0.6 ± 0.2	0.2 ± 0.1
Italy: Tyrrhenian Sea	SL	n/c	n/c
Spain: Balearic Sea	EH	0.3 ± 0.1	0.0 ± 0.0
Tunisia: southern Mediterranean Sea	BB	0.1 ± 0.1	0.3 ± 0.2
	BL	0.4 ± 0.1	0.1 ± 0.1
UK: eastern North Atlantic and North Sea	UK*	0.5 ± 0.2	0.1 ± 0.1

(B)

	ML	GT	VL	PC	SL	EH	BB	BL	UK*
ML		2.0 ± 0.4	2.5 ± 0.5	2.0 ± 0.5	n/c	2.6 ± 0.5	2.2 ± 0.4	2.1 ± 0.4	3.3 ± 0.6
GT	19.5 ± 2.0		1.6 ± 0.4	**0.1 ± 0.1**	n/c	1.7 ± 0.4	**0.3 ± 0.1**	**0.1 ± 0.1**	2.4 ± 0.5
VL	20.1 ± 1.9	18.0 ± 1.9		1.7 ± 0.4	n/c	**0.4 ± 0.1**	1.9 ± 0.4	1.7 ± 0.4	2.9 ± 0.6
PC	19.7 ± 2.0	**0.5 ± 0.1**	18.0 ± 1.9		n/c	1.7 ± 0.4	**0.3 ± 0.1**	**0.2 ± 0.1**	2.5 ± 0.5
SL	19.8 ± 2.0	18.1 ± 1.9	**0.7 ± 0.3**	18.2± 1.9		n/c	n/c	n/c	n/c
EH	19.8 ± 2.0	17.7 ± 1.9	**0.7 ± 0.2**	17.8 ± 1.9	**0.3 ± 0.1**		1.9 ± 0.4	1.7 ± 0.4	3.1 ± 0.6
BB	19.3 ± 2.0	**0.3 ± 0.1**	18.0 ± 1.9	**0.4 ± 0.1**	18.1 ± 1.9	17.7 ± 1.9		**0.2 ± 0.1**	2.7 ± 0.5
BL	19.7 ± 2.0	**0.5 ± 0.1**	18.1 ± 1.9	**0.5 ± 0.1**	18.2 ± 1.9	17.8 ± 1.9	**0.3 ± 0.1**		2.5 ± 0.5
UK*	20.4 ± 2.1	20.7 ± 2.1	21.1 ± 2.1	20.8 ± 2.1	20.8 ± 2.0	20.8 ± 2.0	20.6 ± 2.1	21.0 ± 2.1	

(A) Number of base substitutions per site by averaging over all sequence pairs within each sampling locality group. For each marker, p-distance estimates are reported as percentages with the relative standard error (SE) calculated with a bootstrap procedure (1000 replicates).

(B) Number of base substitutions per site by averaging over all sequence pairs between sampling localities groups. Below the diagonal: *COI* p-distances (%) and relative SE estimates. Above the diagonal: *28S* p-distances (%) and relative SE estimates standard error estimates. Values corresponding to specimens belonging to the same species are in bold. Location codes: BB, Bizerte Bay; BL, Bizerte Lagoon; EH, Empuriabrava Harbour; GT, Gulf of Trieste; ML, Mljet Lakes; PC, Porto Cesareo; SL, Sabaudia Lake; UK, United Kingdom (Southampton, Oban, Orkney and St Andrews); VL, Varano Lagoon.

*UK refers to all the specimens collected around the United Kingdom (Ob, Or, So, and SA).

n/c: not computable (data not available or sample size too small).

stage of *Aurelia* sp. 1 and *Aurelia* sp. 8 (Table 3; SIMPER analysis, Table S2); however, only one feature – either MDD/TBL or StL/TBL, depending on the populations compared (VL and EH, respectively) – distinguishes *Aurelia* sp. 1 from *Aurelia* sp. 8.

In the ephyra stage, the PERMANOVA pairwise test showed that *Aurelia* sp. 1 and *Aurelia* sp. 5 differ significantly from *Aurelia* sp. 8 for two morphological character ratios (LStL/BD, CDD/BD; Tables 3 and S2). The RLL/BD distinguishes *Aurelia* sp. 1 (VL) from *Aurelia* sp. 5 (Table 3), contributing 50% of the observed difference (SIMPER analysis, Table S2).

More species-specific characters were informative in comparisons of the medusa stage. The PERMANOVA pairwise test showed that *Aurelia* sp. 1 is morphologically distinct from *Aurelia* sp. 5 and *Aurelia* sp. 8 for 40 and 17% of the selected characters, respectively (Table 3). Because of the high intraspecific variability of *Aurelia* sp. 1 (67%), characters reliably distinguishing *Aurelia* sp. 1 medusae from *Aurelia* sp. 5 medusae were restricted to manubrium depth, manubrium width, proximal gastric diameter, and rhopaliar and non-rhopaliar indentations (Fig. 5; Tables 3 and S3). Similarly, only non-rhopaliar indentations were reliable in discriminating *Aurelia* sp. 1 from *Aurelia* sp. 8

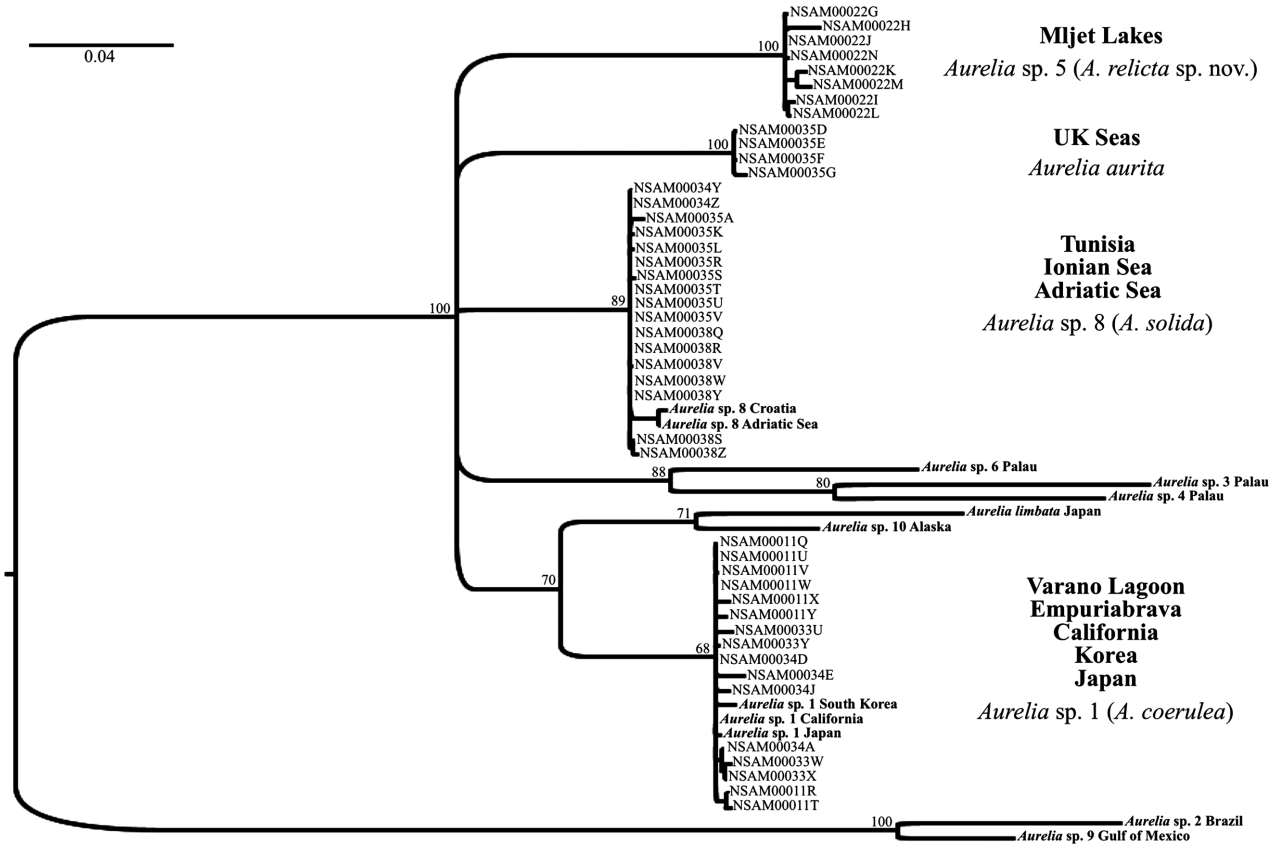

Figure 3. *COI–28S* concatenated maximum-likelihood tree reconstructed using GARLI 2.0. Numbers adjacent to nodes show the bootstrap support values. The scale indicates the number of substitutions per site. Reference sequences from GenBank are in bold.

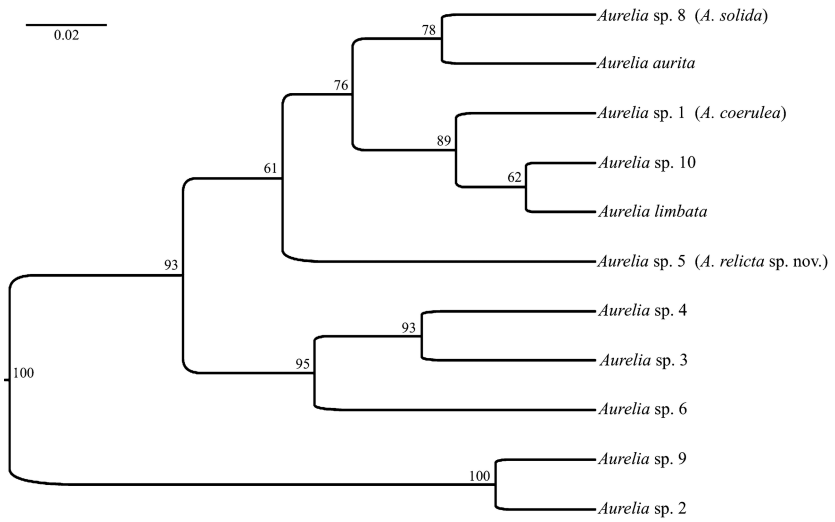

Figure 4. Bayesian species tree estimated using *BEAST (*COI* + *28S*). Numbers adjacent to nodes show the posterior probability values. The scale indicates the estimated number of substitutions per site.

(Fig. 5; Tables 3 and S3). The remaining characters, including the folding of oral arms, oral arm width, distal gastric diameter, bell shape, bell thickness, and anastomoses were inconsistent, and did not reliably distinguish *Aurelia* sp. 1 from *Aurelia* sp. 5 (Fig. 6; Tables 3 and S4).

The highest percentage (53%) of interspecific morphological variation distinguishes *Aurelia* sp. 5 and *Aurelia* sp. 8, and reflects differences in manubrium depth, oral arm length and oral arm width, distal gastric diameter, bell thickness, anastomoses, and rhopaliar indentations (Fig. 5; Tables 3 and S3).

The CAP analysis of morphometric data distinguished among geographical groups of *Aurelia* spp. polyps (tr = 0.92, $P = 0.0002$), ephyrae (tr = 1.46; $P = 0.0002$), and medusae (tr = 2.02, $P = 0.0002$); however, their sorting success is variable, depending on the life stage, with the greatest hit score for medusa characters (88%) followed by ephyra (75%) and polyp (59%) stage characters (CAP analysis, percentage of total correct). The CAP plot for polyps (Fig. 7A) shows an overlap in morphology for *Aurelia* sp. 1, *Aurelia* sp. 5, and *Aurelia* sp. 8: a failure to clearly discriminate between all species. In contrast, in the CAP plot for ephyrae, the first canonical axis had high values of canonical correlations (δ) with the multivariate data, especially with the variable central disc diameter (CDD/BD; $\delta_1 = 0.88$), discriminating between geographical groups and therefore among the ephyra stages of the three species (Fig. 7B).

The CAP plot for medusae also clearly separated different species of *Aurelia*. Further support for the hypothesis of intra- and interspecific differences was given by the value of canonical correlation (δ) of the

Table 2. Diagnostic characters for the three Mediterranean *Aurelia* spp.: A, polyp stage; B, ephyra stage; C, medusa stage

(A)

	Species		
Polyp stage	*Aurelia* sp. 1 (= *A. coerulea*)	*Aurelia* sp. 5 (= *A. relicta* sp. nov.)	*Aurelia* sp. 8 (= *A. solida*)
Polyp length (TBL; mm)	1.74 ± 0.09	2.2 ± 0.1	2.9 ± 0.1
Mouth diameter (MDD: % of BD)	96.81 ± 7.45	77 ± 4.6	59.7 ± 3.6
Hypostome shape and length (HL: % of BD)	Cruciform; 14.25 ± 1.16	Dome shaped; 17.4 ± 1.3	Cruciform; 14.9 ± 1.2
Stalk length (StL: % of BD)	15.55 ± 1.21	17.1 ± 1.8	7.21 ± 1.1
Colour	Pinkish	Whitish–pinkish	Pinkish
No. of tentacles	16–22	16	16
Asexual reproduction strategies	Budding, podocyst, EFSP*, IFSP*	Budding, podocyst, EFSP*, IFSP*, pseudoplanulae	Budding, podocyst
Strobilation	Polydisc, up to 17 discs	Polydisc, up to 15 discs	Polydisc, up to 20 discs

(B)

	Species		
Ephyra stage	*Aurelia* sp. 1 (= *A. coerulea*)	*Aurelia* sp. 5 (= *A. relicta* sp. nov.)	*Aurelia* sp. 8 (= *A. solida*)
Ephyra diameter (BD; mm)	3.72 ± 0.18	3.5 ± 0.2	2.8 ± 0.1
Central disc diameter (CDD: % of BD)	43.93 ± 0.60	40.3 ± 0.3	39.6 ± 0.8
Marginal lappet shape	Breadknife shape to round to oval	Breadknife shape, pointed at tip	Breadknife shape
Lappet proportions			
(LStL: % of BD)	17.28 ± 0.41;	16.8 ± 0.5;	18.7 ± 0.8;
(RLL: % of BD)	11.55 ± 0.44	14.3 ± 0.4	12.2 ± 0.4
Colour	Dark orange, brownish	Milky–transparent	Milky–transparent
No. gastric filaments	0	1–2	1–2

Table 2. *Continued*

(C)

Medusa stage	Species		
	Aurelia sp. 1 (= *A. coerulea*)	*Aurelia* sp. 5 (= *A. relicta* sp. nov.)	*Aurelia* sp. 8 (= *A. solida*)
Umbrella shape, diameter (mm) and thickness	Disc flat, numerous small whitish tentacles arranged slightly above the bell margin;	Disc flat, numerous small whitish tentacles arranged slightly above the bell margin;	Disc rounded and thick, numerous small and pinkish tentacles arranged slightly above the bell margin;
	f1, 101.05 ± 7.32;	f1, 87.10 ± 7.45;	f1, 151.29 ± 4;
	f22, 0.13 ± 0.01	f22, 0.10 ± 0.01	f22, 0.15 ± 0.01
Manubrium shape, depth, and width (% of BD)	Cruciform, rigid, large;	Cruciform, rigid;	Cruciform, rigid;
	f2, 6.05 ± 0.75;	f2, 1.45 ± 0.12;	f2, 3.39 ± 0.51;
	f6, 17.25 ± 0.54	f6, 13.87 ± 0.67	f6, 14.88 ± 0.66
Oral arms shape, length, and width (% of BD)	Folded;	Slightly folded;	Slightly folded;
	f5, 40.17 ± 1.5;	f5, 38.85 ± 2.44;	f5, 44.49 ± 1.32;
	f7, 9.25 ± 0.4	f7, 7.76 ± 0.85	f7, 10.46 ± 0.83
Gastric pouch shape and size (% of BD)	Gastric cavities distant,	Gastric cavities close,	Gastric cavities close,
	f9, 14.55 ± 0.60;	f9, 10.31 ± 0.60;	f9, 11.43 ± 0.86;
	f10, 35 ± 1.15;	f10, 30.83 ± 0.66,	f10, 42.81 ± 1.77;
	f11, 2.95 ± 0.35	f11, na	f11, 2.9 ± 0.23
Colour of gastric filaments, gonads, and bell	f14, f15, pinkish; f17, whitish	f14, f15, f17, whitish	f14, f15, rose–violet; f17, salmon–light violet
No. of lobes;	f19, 8 or 16;	f19, 8;	f19, 8;
No. of rhopalia	f20, 8	f20, 8	f20, 8
Shape of sense organ, rhopaliar and non-rhopaliar indentations (% of BD)	Sense organ protected on the exumbrellar side by a triangular dorsal hood with rhopalia directed towards bell margin;	Sense organ protected on the exumbrellar side by a triangular dorsal hood with rhopalia directed towards bell margin;	Sense organ protected on the exumbrellar side by a dorsal hood with a rhomboidal oval shape with rhopalia directed towards exumbrella;
	f29, 3.51 ± 0.22;	f29, 5.06 ± 0.27;	f29, 3.47 ± 0.1;
	f30, 1.02 ± 0.09	f30, 1.68 ± 0.13	f30, 1.75 ± 0.16
Number of origins of canals	f23 + f24 + f25, 7–10	f23 + f24 + f25, 6–9	f23 + f24 + f25, 6–9
Anastomoses	f6, f27, f28, all canals anastomose	f6, f27, f28, all canals anastomose	f6, f27, f28, all canals anastomose

For character acronyms, see Figure 2.
Data expressed as means of values recorded (± SDs). Each population comprised 30 polyps, six ephyrae (at time 0), and between seven and ten medusae.
*EFSP; external free-swimming propagules; IFSP, internal free-swimming propagules.
na, not available (medusae not reproductively mature).

first axis ($\delta_1 = 0.88$), which is best represented by the variable folding of oral arms (f3). The ordination pattern of the third canonical variable along the *y*-axis was also significant ($\delta_2 = 0.77$), with correspondence in the variable oral arm width (f7). Above all, the variables rhopaliar and non-rhopaliar indentations grouped, respectively, all specimens of *Aurelia* sp. 5 and *Aurelia* sp. 8, and consequently separated the species (Fig. 7C). The variables manubrium depth and manubrium width, folding of oral arms,

Table 3. PERMANOVA pair-wise test on morphometrics data in *Aurelia* spp. polyps, ephyrae, and medusae

Species	Morphometric characters
Polyp stage	
Aurelia coerulea (EH)–*Aurelia coerulea* (VL)	MDD/TBL (0.001), HL/TBL (0.017), StL/TBL (0.001)
Aurelia coerulea (EH)–***Aurelia relicta* sp. nov.** (ML)	MDD/TBL (0.005), HL/TBL (0.003), StL/TBL (0.033)
Aurelia coerulea (VL)–***Aurelia relicta* sp. nov.** (ML)	MDD/TBL (0.001), StL/TBL (0.02)
Aurelia coerulea (EH)–*Aurelia solida* (GT)	StL/TBL (0.001)
Aurelia coerulea (VL)–*Aurelia solida* (GT)	MDD/TBL (0.001)
***Aurelia relicta* sp. nov.** (ML)–*Aurelia solida* (GT)	MDD/TBL (0.007),StL/TBL (0.001)
Ephyra stage	
Aurelia coerulea (EH)–*Aurelia coerulea* (VL)	CDD/BD (0.003), RLL/BD (0.016)
Aurelia coerulea (EH)–***Aurelia relicta* sp. nov.** (ML)	–
Aurelia coerulea (VL)–***Aurelia relicta* sp. nov.** (ML)	RLL/BD (0.004)
Aurelia coerulea (EH)–*Aurelia solida* (GT)	CDD/BD (0.006), LStL/BD (0.004)
Aurelia coerulea (VL)–*Aurelia solida* (GT)	CDD/BD (0.002), LStL/BD (0.004)
***Aurelia relicta* sp. nov.** (ML)–*Aurelia solida* (GT)	CDD/BD (0.002), LStL/BD (0.024)
Medusa stage	
Aurelia coerulea (EH)–*Aurelia coerulea* (VL)	f3 (0.0012), f5 (0.0316), f7 (0.0112), f10 (0.0004), f11 (0.0246), f12 (0.0003), f13 (0.001), f19 (0.0438), f22 (0.0204), f26 (0.0034), f27 (0.0204), f28 (0.0426)
Aurelia coerulea (EH)–***Aurelia relicta* sp. nov.** (ML)*	f2 (0.0002), f6 (0.016), f9 (0.0002), f22 (0.0176), f26 (0.0002), f27 (0.0006), f28 (0.0016), f29 (0.0002), f30 (0.0004)
Aurelia coerulea (VL)–***Aurelia relicta* sp. nov.** (ML)*	f2 (0.0002), f3 (0.002), f6 (0.0012), f7 (0.0212), f9 (0.0036), f10 (0.0002), f19 (0.0294), f21 (0.0002), f27 (0.0386), f29 (0.0002), f30 (0.0188)
Aurelia coerulea (EH)–*Aurelia solida* (GT)	f5 (0.001), f7 (0.0038), f9 (0.0104), f10 (0.0006), f13 (0.0104), f26 (0.0218), f29 (0.0024), f30 (0.0014)
Aurelia coerulea (VL)–*Aurelia solida* (GT)	f2 (0.0192), f3 (0.0004), f6 (0.01), f10 (0.0068), f12 (0.0002), f13 (0.0308), f21 (0.0438), f22 (0.006), f30 (0.0024)
***Aurelia relicta* sp. nov.** (ML)*–*Aurelia solida* (GT)	f2 (0.002), f5 (0.0056), f7 (0.0066), f10 (0.0006), f22 (0.0088), f26 (0.0096), f27 (0.0162), f29 (0.0112)

P values, based on PERMANOVA (perm) methods, depending upon the number of unique permutations (999), are indicated in brackets. Abbreviations for polyps: HL, hypostome length; MDD, mouth disc diameter; StL, stalk length; TBL, total body length. Abbreviations for ephyrae: BD, bell diameter; CDD, central disc diameter; LStL, lappet stem length; RLL, rhopalial lappet length. Location codes: EH, Empuriabrava Harbour; GT, Gulf of Trieste; ML, Mljet Lakes; VL, Varano Lagoon.

Aurelia coerulea (= *A.* sp. 1), ***Aurelia relicta* sp. nov.** (= *A.* sp. 5), *Aurelia solida* (= *A.* sp. 8).

*The characters f11, f12, and f13 were not considered in the comparison with ***Aurelia relicta* sp. nov.** because of the immaturity of the medusae.

proximal gastric diameter, and bell shape distinguished *Aurelia* sp. 1 (Fig. 7C).

Development of gastric system in *Aurelia* spp. ephyrae

All specimens belonging to the same population ($N = 6$ for each population) showed a consistent pattern of development over 4 weeks. At liberation (time 0), rhopalial canals were spade-like to slightly forked in each ephyra population (Fig. 8). Velar canals were not well developed and all appeared unforked. The statocysts appeared bright yellow and the mouth was cruciform in all populations. The number of gastric filaments per quadrant was consistently zero for *Aurelia* sp. 1, and one or two for *Aurelia* sp. 5 and *Aurelia* sp. 8.

After 1 week of development, rhopalial canals maintained the same shape as observed at time 0. Spade-like velar canals became noticeable, and were slightly rhombic in the EH population. Pointed lappets became visible in *Aurelia* sp. 5, whereas they appeared breadknife-shaped to round to oval in *Aurelia* sp. 1. In all species, slightly rounded lips developed on the cruciform mouth of the ephyrae, as well as two gastric filaments per quadrant of each ephyra.

By the second week, the colour of ephyrae faded and became transparent. The rhopalial canals

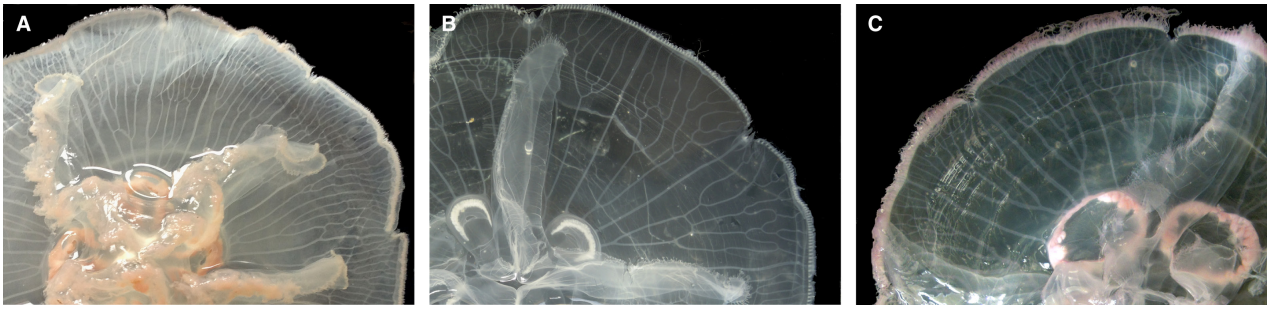

Figure 5. Interspecific morphological differences in the anastomoses and bell indentations: A, *Aurelia coerulea* (= *Aurelia* sp. 1), female, bell diameter (BD) = 125 mm; B, ***Aurelia relicta* sp. nov.** (= *Aurelia* sp. 5), immature specimen, BD = 95 mm; C, *Aurelia solida* (= *Aurelia* sp. 8), male, BD = 160 mm.

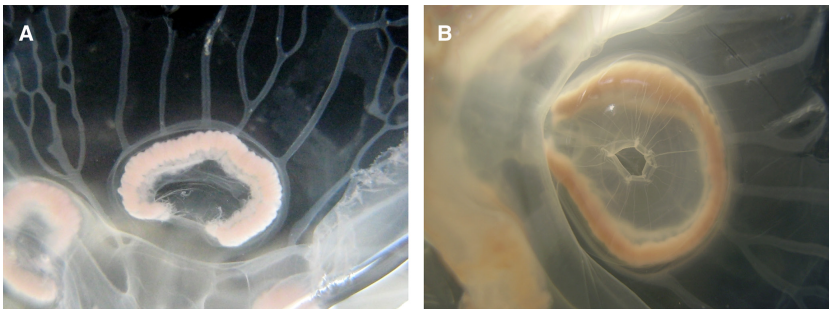

Figure 6. Ontogenetic variation in subgenital pore size (f11) and position (f12) in male specimens of *Aurelia coerulea* from: A, Empuriabrava Harbour (EH), bell diameter (BD) = 63 mm; B, Varano Lagoon (VL), BD = 120 mm.

maintained their shape whereas velar canals elongated and formed side branches (Fig. 8C, H, M, R). Velar lappets appeared between the marginal lappets. The shape of lappets clearly became oval and spoon-like in *Aurelia* sp. 1 and *Aurelia* sp. 8 (Fig. 8C, H, R), or became slightly pointed and spoon-like in *Aurelia* sp. 5 (Fig. 8M). In all samples, the manubrium grew and the number of gastric filaments increased again, reaching between four and eight per quadrant (Fig. 8).

In the third week lappets turned into a rounded spoon-like shape in all *Aurelia* species (Fig. 8D, I, N, S). Rhopalial canals became slightly forked, grew and fused with velar canals, originating a primary ring canal, almost complete in *Aurelia* sp. 1 (Fig. 8D, I), but still developing in *Aurelia* sp. 5 and *Aurelia* sp. 8 (Fig. 8 N, S). In all populations, the oral arms continued their extension from the manubrium, and the gastric filaments increased in number (to more than eight per quadrant). Tentacular bulbs appeared in each population except in EH.

In week 4, in *Aurelia* sp. 5 and the *Aurelia* sp. 1 populations of VL, new centripetal canals originated from the ring canal and tentacles developed from the bulbs. Tentacular bulbs also appeared in the *Aurelia* sp. 1 population of EH. The shape of lappets and rhopalial canals did not vary and the ring canal was complete in all populations (Fig. 8E, J, O, T), and oral arms were now clearly distinct. The gastric filaments grouped and outlined the primordial shape of gastric pouches in *Aurelia* sp. 5 and *Aurelia* sp. 1 populations of VL (Fig. 8J, O).

SYSTEMATIC ACCOUNT AND DESCRIPTION OF THREE MEDITERRANEAN SPECIES OF *AURELIA*

The morphological and molecular analyses allowed the consistent identification of three species of *Aurelia* in the Mediterranean Sea (see below). By literature-based morphological comparison, known distribution range, and putative geographical origin, two clades (*Aurelia* sp. 1 and *Aurelia* sp. 8) can be referred to existing valid species, *Aurelia coerulea* von Lendenfeld, 1884 and *Aurelia solida* Browne, 1905. The third clade (*Aurelia* sp. 5) must be described as a new species: *Aurelia relicta* sp. nov.

Order Semaeostomeae L. Agassiz, 1862
Family Ulmaridae Haeckel, 1880

Semaeostomeae with simple or branched radial canals and a ring canal; with or without subgenital pits.

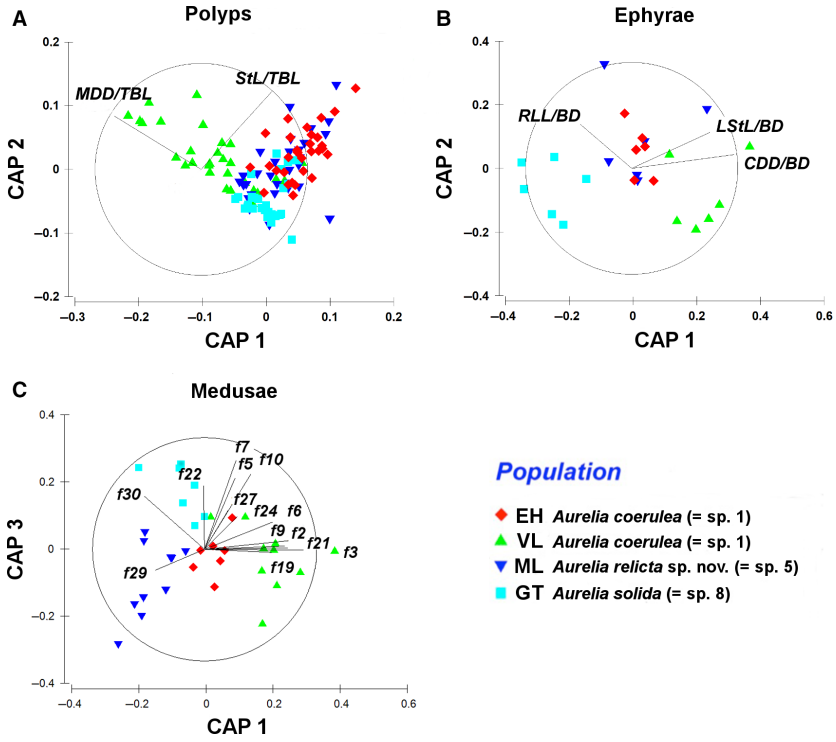

Figure 7. Canonical analysis of principal coordinates (CAP) bi-plot ordination (based upon a Euclidean distance similarity matrix) showing canonical axes (CAP1, CAP2) that best discriminate *Aurelia* spp. populations: A, polyps; B, ephyrae; and C, medusae. The correlation with canonical axes are only shown when the Pearson's correlation coefficient is >0.4. The length of each vector line is proportional to the strength of the correlation.

Genus *Aurelia* Lamarck, 1816

Diagnosis: Ulmaridae with small marginal tentacles, and lappet-like structures arising from exumbrella slightly above umbrella margin. Umbrella margin divided by eight or 16 marginal clefts; four unbranched oral arms; anastomoses between a few or all of the radial canal branches.

Type species: Aurelia aurita (Linnaeus, 1758).

Aurelia coerulea von Lendenfeld, 1884

Aurelia coerulea von Lendenfeld, 1884: 280–281. Type locality: Port Jackson, Australia.
Aurelia japonica Kishinouye, 1891: 289–291, fig. unnumbered. Type locality: Tokyo Bay, Japan.
Aurelia sp. 1 Dawson & Jacobs, 2001: 93 (Newport Beach, California, USA). Dawson, 2003: 375–376 (Tokyo Bay, northern Japan, Australia, Atlantic, Mediterranean coast of France, and east coast of USA).
Aurelia UBI lineage Schroth *et al.*, 2002: 4 (table 2) (California, USA; Atlantic and Mediterranean coasts of France; Australia, Indian Ocean; Japan).

Material examined: Holotype: Female medusa, VL, 13 September 2011, 132 mm BD, deposited in UNIPD. Accession number: CN56CH.

Paratype I: Female medusa, VL, 13 September 2011, 136 mm BD, deposited in UNIS_SCY. Accession number: UNIS_SCY_011.

Paratype II: Female medusa, EH, 15 October 2013, 85 mm BD, deposited in UNIS_SCY. Accession number: UNIS_SCY_012.

Other material: Eight medusae, VL, 13 September 2011, 107–143 mm BD deposited in UNIS_SCY. Accession numbers: UNIS_SCY_013–020.

Other material: Seven medusae, EH, 15 October 2013, 38–80 mm (range of BD) deposited in UNIS_SCY. Accession numbers: UNIS_SCY_021–027. Specimens of polyps and ephyrae were examined but not preserved nor registered.

Description (based on holotype and paratypes): Morphometric and meristic data for polyp and ephyra stages are shown in Table 2. Morphology is illustrated in Figures 5A, 6, 8A–J, 9A, B, 10A, B, and 11A–D. Molecular diagnosis is presented in Figures 3 and 4.

Polyp: Tentacles 16–22. Tentacle diameter uniform or slightly decreasing along the proximal–distal axis.

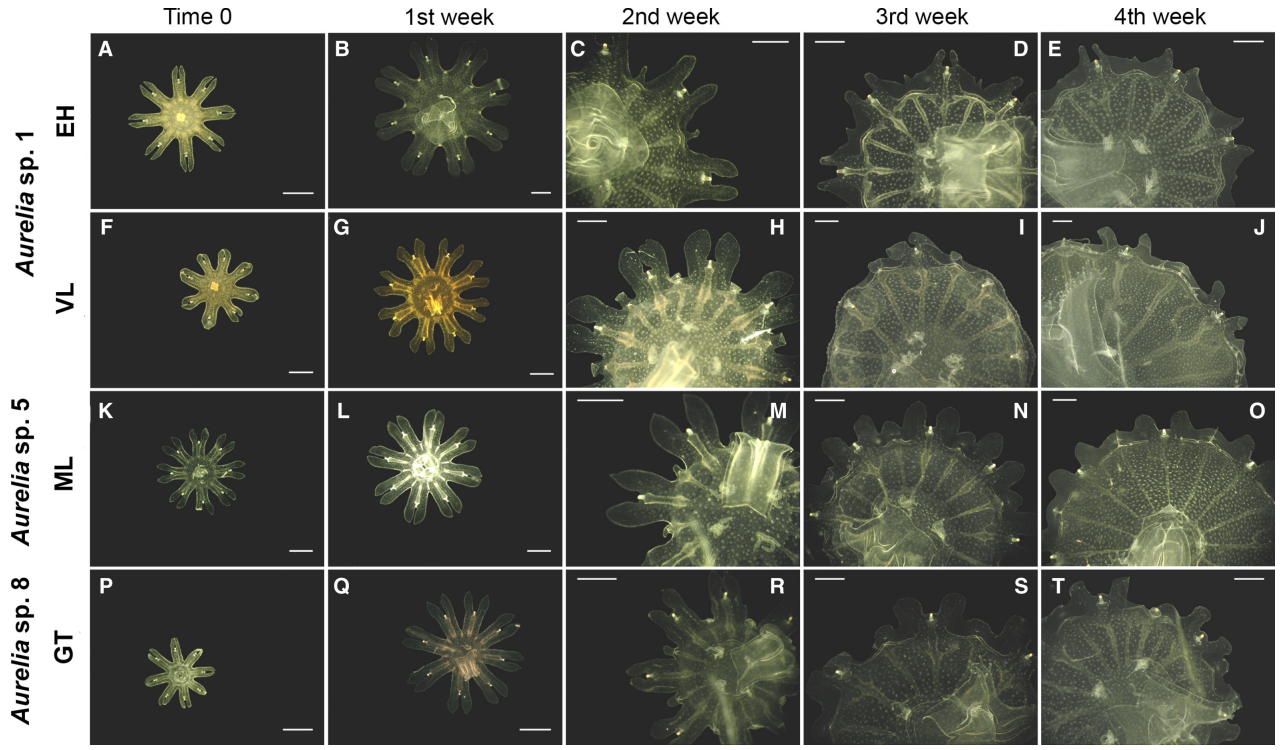

Figure 8. Development of the gastric system in *Aurelia* ephyrae from four Mediterranean locations, reared in the laboratory: A–E, *Aurelia coerulea* (= *Aurelia* sp. 1), EH; F–J, *Aurelia coerulea* (= *Aurelia* sp. 1), VL; K–O, ***Aurelia relicta* sp. nov.** (= *Aurelia* sp. 5), ML; P–T, *Aurelia solida* (= *Aurelia* sp. 8), GT. Scale bars: 1 mm.

Hypostome cruciform (Figure 9A, B). Colour pinkish. Asexual reproduction by budding from stolon (Fig. 10A) or directly from the column of parental polyp. Rarely podocyst originates at the base of pedal disc or along the stolon. External free-swimming propagules (EFSPs) and internal free-swimming propagules (IFSPs; Vagelli, 2007) observed, with EFSP more common (Fig. 10B). Strobilation polydisc, with up to 17 discs observed.

Ephyra: Normally eight arms, 16 marginal lappets, and eight rhopalia. Marginal lappets with breadknife-like shape (Fig. 8A, F), both margins rounded, or sharpened (internal margin, rhopaliar side). Dark orange–brownish. Young ephyrae: without gastric filaments at liberation. Manubrium cruciform and oral arms developing during the second week (Fig. 8C, H).

Medusa: Disc flattened, up to 26 cm BD. Bell shape typically concave, or undulating, eight marginal lobes (occasionally 16 when BD > 11 cm), eight marginal rhopalia in shallow clefts (f29, 3.5 ± 0.35 mm), but deeper than non-rhopalial clefts (if present), where the adradial canals join the bell margin.

Sense organ protected on the exumbrellar side by a triangular dorsal hood (Fig. 11A). Long rhopalium directed towards the bell margin (Fig. 11B). The ectodermal ocellus is a small protuberance with a dense concentration of reddish pigment granules (Fig. 11C). A large endodermal ocellus on the subumbrellar side at the base of lithocyst (Fig. 11C) with reddish pigment granules arranged in a circular shape around the perimeter (Fig. 11D).

Numerous small whitish tentacles arranged slightly above the bell margin. Manubrium cruciform, rigid, large, 2–14 mm depth, width 8–28 mm, bearing four perradial, folded oral arms, with mean length (f5) 4*r*/5.

Four (occasionally between five and seven) interradial gonads, horseshoe-shaped. Planulae brooded on the oral arms. Relative to the gastric tissue, the subgenital pore is placed centrally to or, in smaller medusae, adjacent to but circumscribed by the gastric filaments (Fig. 6). Subgenital pore diameter (f11) 1–6 mm. Opposite gastric cavities distant across the diameter. Gastric diameter highly variable: proximal (f9) ranging from *r*/6 to *r*/3; distal (f10) ranging from *r*/2 to 6*r*/7. From each gastrogenital sinus between seven and ten broad canals depart (range of variation: two or three perradials, two or three adradials, and three or four interradials). Interradial and perradial canals branched, frequently anastomosed in the second and third distal

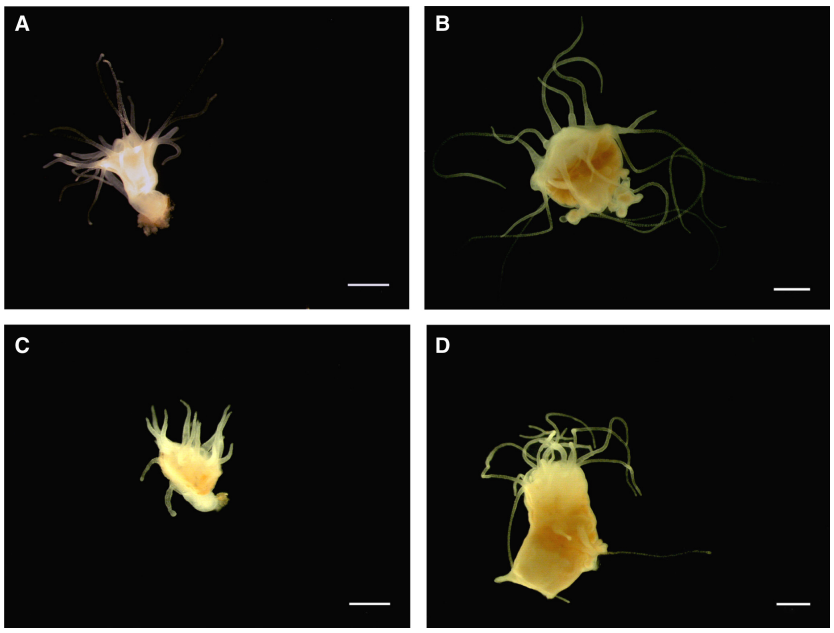

Figure 9. Morphology of *Aurelia* spp. polyps: A, *Aurelia coerulea* (= *Aurelia* sp. 1), EH; B, *Aurelia coerulea* (= *Aurelia* sp. 1),VL; C, ***Aurelia relicta* sp. nov.** (= *Aurelia* sp. 5), ML; D, *Aurelia solida* (= *Aurelia* sp. 8), GT. Scale bars: 1 mm.

of the bell. Number of perradial (f26) and interradial (f27) anastomoses: 14–48 and 13–51, respectively. Adradial canals (f28) mostly unbranched, moderately connected to the canal mesh both in the distal or proximal portion (Fig. 5A).

Type locality: Port Jackson (Australia).

Habitat: In the Mediterranean Sea, apparently restricted to euryhaline and eurythermal coastal lagoons, marinas, and harbours.

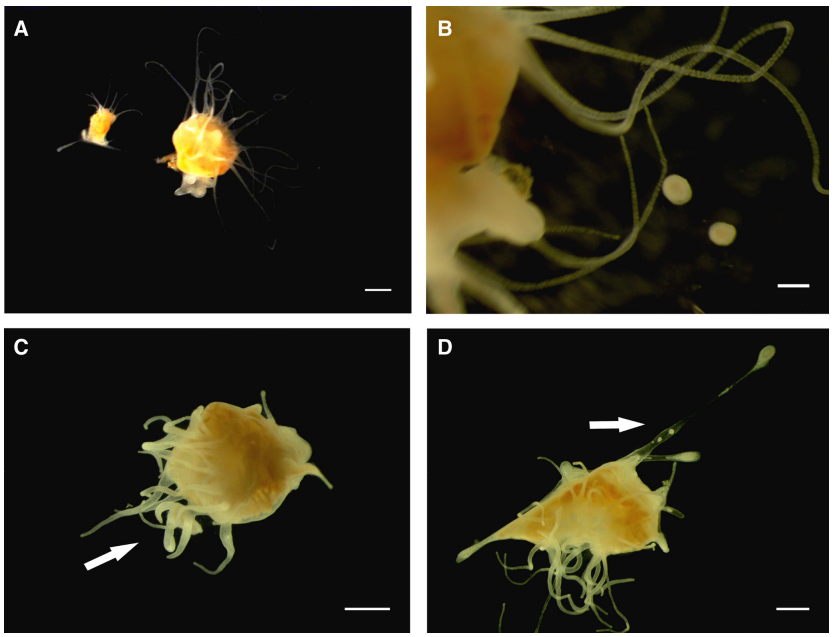

Figure 10. Some asexual reproduction strategies in *Aurelia* spp. polyps: A, directed budded polyp in *Aurelia coerulea* (= *Aurelia* sp. 1); B, free-swimming buds in *Aurelia coerulea* (= *Aurelia* sp. 1); C, polyp budded on tentacle in ***Aurelia relicta* sp. nov.** (= *Aurelia* sp. 5); D, internal free propagules in ***Aurelia relicta* sp. nov.** (= *Aurelia* sp. 5). Scale bar: A–C, 1 mm; D, 0.5 mm.

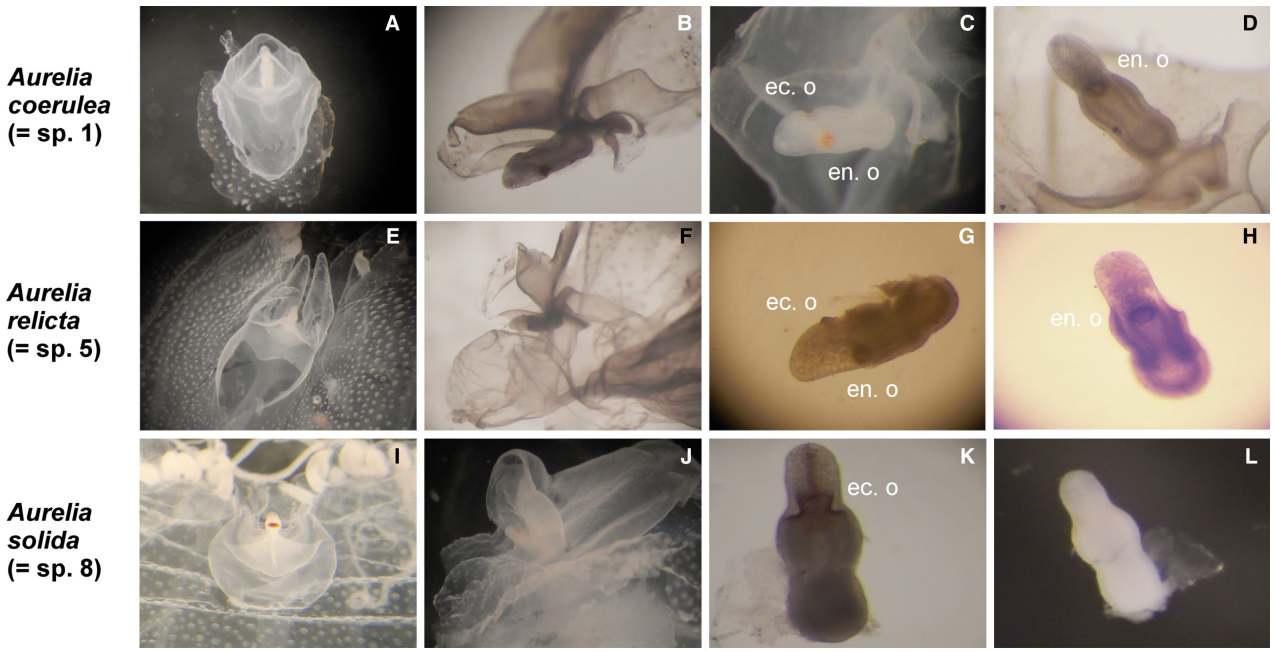

Figure 11. Structure of marginal sense organ in *Aurelia* medusae: A–D, *Aurelia coerulea* (= *Aurelia* sp. 1), bell diameter (BD) = 136 mm; E–H, ***Aurelia relicta* sp. nov.** (=*Aurelia* sp. 5), BD = 95 mm; I– L, *Aurelia solida* (= *Aurelia* sp. 8), BD = 144 mm. The rhopalium is directed towards the bell margin in *A. coerulea* (B) and ***A. relicta* sp. nov.** (F), angled at ~90° in *A. solida* (J). Abbreviations: ec. o, ectodermal ocellus; en. o, endodermal ocellus.

Distribution in the Mediterranean Sea: Including at least VL (Adriatic Sea), EH (Balearic Sea), and SL (Thyrrenian Sea).

Distribution outside the Mediterranean Sea: Reported from Japan (Miyazu Bay, Sakata Bay, Uwa Bay, Ondo Strait, Tokyo Bay), Korea (Incheon, Geojedo, Busan), California (Long Beach, Marina del Rey, Newport Beach, San Diego), and numerous sites throughout the Australian coast, from Queensland to New South Wales and Western Australia (Dawson & Jacobs, 2001; Dawson, 2003; Ki *et al.*, 2008). Few DNA sequences clustering into the *A. coerulea* clade were previously obtained from samples collected in the eastern Atlantic and Mediterranean coastal areas of France (Schroth *et al.*, 2002).

Remarks: Within the genus *Aurelia*, *A. coerulea* is the taxon with the broadest world distribution. The type locality is not coincident with its inferred biogeographic origin of the Western Pacific coastal waters (Dawson *et al.*, 2005). The name *A. coerulea* has priority over its junior synonym *Aurelia japonica* (Kishinouye, 1891).

AURELIA RELICTA SCORRANO, AGLIERI, BOERO, DAWSON & PIRAINO SP. NOV.

Aurelia sp. Benović *et al.*, 2000: 202, fig. 7 (Mljet lakes, Croatia).

Aurelia sp. 5 Dawson & Jacobs, 2001: 93 (Mljet). Ramšak *et al.*, 2012: 70 (South Adriatic, Mljet lakes). *Aurelia* MS-MKL lineage Schroth *et al.*, 2002: 4 (table 2) (Mljet lakes, Croatia).

Material examined: Holotype: Immature, ML, June 2013, 76 mm BD. Deposited in UNIPD. Accession number: CN57CH.

Paratype I: Immature, ML, June 2013, 66 mm BD. Accession number: UNIS_SCY_028.

Paratype II: Immature, ML, June 2013, 68 mm BD. Accession number: UNIS_SCY_029.

Other material: Six medusae, ML, June 2013, 58–130 mm (range of BD); three medusae, ML, February 2013, 70–95 mm (range of BD). Accession numbers: UNIS_SCY_030–038.

Description (based on holotype, paratypes, with additional data on mature jellyfish from Benović et al., 2000): Morphometric and meristic data for polyp and ephyra stages are presented in Table 2. Morphology is illustrated in Figures 5B, 8K–O, 9C, 10C, D, and 11E–H. Molecular diagnosis is presented in Figures 3 and 4.

Polyp: Tentacles typically 16. Only two polyps (out of 30) with 14 and 22 tentacles observed. Tip of tentacles thickened. Hypostome dome-shaped. Colour whitish–pinkish.

Main asexual reproduction by budding from stolon or directly from the column of parental polyp. Rarely podocyst originates at the base of pedal disc or along the stolon. Ciliated IFSPs (from gastrovascular cavity or stolon) frequently liberated (Fig. 10D, arrow), exhibiting a slight rotatory (planula-like) movement for 1–3 days, before final settlement and development into polyp. EFSPs also observed. Asexual reproduction also through pseudoplanulae (Fig. 10C, arrow; Hérouard, 1909; Piraino *et al.*, 2004). Strobilation polydisc, up to 15 discs observed.

Ephyra: Normally eight arms, 16 marginal lappets, and eight rhopalia. Marginal lappets long, breadknife-like shaped (Straehler-Pohl & Jarms, 2010), pointed at tip (Fig. 8K). Colour milky–transparent. Manubrium cruciform, oral arms appearing during the second week of ephyra development. One or two gastric filaments per quadrant.

Medusa: Disc flat, whitish. Benović *et al.* (2000) reported BD up to 55 cm in diameter. Bell shape (f21), typically undulating or straight, with eight marginal lobes and eight marginal sense organs in a medium cleft (f29, 4.32 ± 0.3 mm).

The sense organ is protected on the exumbrellar side by a dorsal hood of triangular shape (Fig. 11E). The rhopalium is long and directed towards the bell margin (Fig. 11F). Long rhopaliar lappets are visible on both exumbrellar and sumbumbrellar sides (Fig. 11E).

The ectodermal ocellus is small and appears as a protuberance with a dense concentration of reddish pigment granules (Fig. 11G). A large endodermal ocellus is visible on the subumbrellar side at the base of the lithocyst (Fig. 11G). The reddish pigment granules of the endodermal ocellus are arranged in a circular shape, with the dark reddish pigment granules around the perimeter (Fig. 11H).

The sense organ is always surrounded by two thin branches of medium interradial canal, which turn into anastomoses (or not) with close canals in larger individuals.

Numerous small and whitish tentacles arranged slightly above the bell margin. Manubrium cruciform, rigid, depth 1–3 mm, width 8–21 mm, with four perradial oral arms slightly folded, mean length (f5) 7*r*/9.

Four interradial gonads, horseshoe-shaped. Opposite gastric cavities close across the diameter; proximal gastric diameter (f9) ranging from *r*/7 to *r*/4; distal gastric diameter (f10) ranging from *r*/2 to 2*r*/3. From each gastrogenital sinus, between six and nine thin canals (see also the development of canals in Fig. 8O) depart (ranges of variation: between two and four perradials, two adradials, and between one and five interradials). Perradial (f26) and interradial (f27) canals gradually branching and anastomosing (between ten and 27 times) in the distal third of the bell, creating a delicate mesh net. Adradial canals (f28) unbranched, occasionally one or two anastomoses are found.

Etymology: From the Latin *relictus* = abandoned, forsaken. The specific name refers to the 'relict' geographic isolation of this species.

Type locality: Veliko Jezero (Mljet Island, Adriatic Sea).

Habitat: Marine, neritic.

Distribution: Currently known from the type locality only.

Remarks: Within the genus *Aurelia*, *Aurelia relicta* sp. nov. has the smallest known distribution.

Aurelia solida Browne, 1905

Aurelia solida Browne, 1905: 960–962, pl. 94, figs 1–2. Type locality: Maldives.
Aurelia TET lineage Schroth *et al.*, 2002: 3, 4 (table 2) (Red Sea, Mediterranean Sea). *Aurelia* sp. 8 Dawson *et al.*, 2005: 11970, fig. 1 (Adriatic, Mediterranean, Red Sea). Ramšak *et al.*, 2012: 70 (North Adriatic, Mediterranean Sea).

Material examined: Holotype: Female, GT, March 2015, 24 cm BD. Deposited in UNIPD. Accession number: CN58CH.

Paratype I: Female, GT, March 2015, 150 mm BD. Accession number: UNIS_SCY_038.

Other material: Seven medusae, GT, March 2015, 134–220 mm (range of BD); one medusa, PC, April 2013, 218 mm BD. All specimens deposited in UNIS_SCY. Accession numbers: UNIS_SCY_039–046.

Description (based on holotype and paratypes): Morphometric and meristic data of polyp and ephyra stages are presented in Table 1. Morphology is illustrated in Figures 5C, 8P–T, 9D, and 11I–L. Molecular diagnosis is presented in Figures 3 and 4.

Polyp: Number of tentacles variable, commonly 16–22, rarely 14. Tentacles ramified in 40% of polyps. Hypostome cruciform. Colour pinkish.

Asexual reproduction by budding from stolon or directly from column of parental polyp. Podocysts also observed. Strobilation polydisc, up to 20 discs observed.

Ephyra: Normally eight arms, 16 marginal lappets, and eight rhopalia. Marginal lappets long, breadknife-like shaped (Straehler-Pohl & Jarms, 2010; Fig. 8P). Colour milky–transparent. Manubrium cruciform. One or two gastric filaments per quadrant.

Medusa: Disc rounded, thick, up to 24 cm in diameter. Bell margin salmon–light violet, bell shape (f21) typically undulating, with eight marginal lobes and eight marginal sense organs in a deep cleft (f29, 5.26 ± 0.2 mm). The sense organ is protected on the exumbrellar side by a dorsal hood of rhomboidal–oval shape (Fig. 11I). The rhopalium is short and directed mostly towards the exumbrellar side, approximately angled at 90° with respect to the direction of rhopalia described in *A. coerulea* and *A. relicta* sp. nov. (Fig. 11J), where rhopalia are directed towards the bell margin. The same pattern was described in the original description given by Browne (1905), in comparison with *A. aurita*.

A large ectodermal ocellus is visible. The reddish pigment granules are arranged in a top-hat shape, with a middle row projecting towards the upper end (Fig. 11K). No endodermal ocellus was detectable on the subumbrellar side (Fig. 11L).

Numerous small and pinkish tentacles are arranged slightly above the bell margin. Manubrium cruciform, rigid, depth 4–8 mm, width 21–27 mm, with four perradial oral arms slightly folded, mean length (f5) 8*r*/9.

Four interradial gonads, horseshoe-shaped, rose–violet. Subgenital pore placed centrally, diameter (f11) ranging from 3.5 to 5.6 mm. Opposite gastric cavities close across the diameter, mean proximal gastric diameter (f9) from *r*/6 to *r*/3, distal gastric diameter (f10) from 3*r*/4 to *r*. From each gastrogenital sinus, between six and nine canals depart (ranges of variation: two or three perradials, between one and three adradials, and between two and four interradials). Canals salmon–violet. Adradial canals (f28) branched a few times, interradial (f26) and perradial canals (f27) branched up to 36 times.

Type locality: Maldive islands (Arabian Sea, Indian Ocean).

Habitat: Marine, open sea. Only one record from coastal lagoon in the Mediterranean Sea.

Distribution in the Mediterranean Sea: Bizerte Bay and Lagoon (Tunisia), Gulf of Trieste (North Adriatic sea), Porto Cesareo (Ionian Sea), Cannes (France).

Distribution outside Mediterranean Sea: Arabian Sea, Red Sea, Maldive Islands, Indian Ocean (Schroth *et al.*, 2002; Dawson *et al.*, 2005; Ramšak *et al.*, 2012).

Remarks: Migration through the Suez Canal and shipping from the Indian Ocean seem to be the most conceivable sources of introduction and spread in Mediterranean open-water areas (Dawson *et al.*, 2005).

DISCUSSION

Towards a validation of characters: a unified, integrative taxonomy

To date, the diversity of moon jellyfishes, genus *Aurelia*, revealed by molecular data has not been reflected in coherent morphological descriptions of any species. The reasons are manifold, including the need to measure the same suites of characters with the same methods in populations across a wide geographic range (including type localities) to reconcile molecular with traditional morphological identifications (Dawson, 2003). Many of the taxonomic characters (i.e. colour, shape characteristics of manubrium, bell, lobes) considered in previous studies (Mayer, 1910; Kramp, 1961; Russell, 1970) were insufficient – either insufficiently variable or inconsistently variable – to discriminate between species (e.g. Dawson, 2003), resulting in many cryptic or 'bad' species, possibly also as a consequence of the spread of parataxonomic approaches (or 'non-professional taxonomists' *sensu* Fontaine *et al.*, 2012).

If these tools were not able to answer the key question regarding this well-known genus, then the costs/benefits for finding scyphystoma polyps justifies the few studies drawing attention to the morphology of the other life stages (Uchida & Nagao, 1963; Straehler-Pohl & Jarms, 2010; Straehler-Pohl *et al.*, 2011; Gambill & Jarms, 2014). Whereas molecular methods have demonstrated the occurrence of multiple species of *Aurelia* worldwide (Dawson & Jacobs, 2001; Schroth *et al.*, 2002; Ramšak *et al.*, 2012), molecular analyses alone, i.e. uncoupled from morphological analysis of voucher specimens, cannot address the validity of species names, descriptions, or types. When molecular and morphological analyses are combined in a modern taxonomic screening of several *Aurelia* spp., covering the entire life cycle and not just adult medusa, we find the expected benefits, manifesting in three major results: (1) we identified three cryptic molecular species of *Aurelia* jellyfish with a heterogeneous distribution across the Western Mediterranean, and Ionian and Adriatic seas; (2) we redescribed two known species, *A. coerulea* and *A. solida*, and newly described the morphological species *A. relicta* sp. nov. from Mljet;

and (3) as a corollary, molecular data for three previously described molecular species (*Aurelia* sp. 1, *Aurelia* sp. 5, and *Aurelia* sp. 8, respectively; Dawson & Jacobs, 2001) are now linked to voucher specimens, holotypes, and paratypes of named taxa.

The species resolution is the product of a process that sees key characters reshuffled in the 'diagnostic' character set, first according to life-history stage, and then according to the species compared. To start, the high intraspecific polymorphism encountered in polyps of *A. coerulea* reduces the usefulness of characters that are not diagnostic because of heritable variation and/or ecophenotypic plasticity of the polyps. Conversely, the shape of the rhopalial lappets of ephyrae and their relative proportions, which are already known to be relevant characters for genus- and family-level identification (Gröndahl & Hernroth, 1987; Straehler-Pohl & Jarms, 2010), also appear to be useful in consistently reflecting specific differences across the three investigated Mediterranean *Aurelia* clades [as also implied for *Aurelia*, *Cyanea*, and *Rhizostoma* in Straehler-Pohl & Jarms (2010: table 3), albeit in the absence of quantitative statistical analyses]. Whether this result is broadly generalizable to other species is unclear, however. To reliably resolve the taxa in any analysis, the number of characters and character states must outnumber the number of taxa, and for statistical phylogenetic confidence the number of characters and states must be several-fold higher than the number of taxa (Felsenstein, 1985; Dawson, 2003). With only a handful of putatively independent characters in the polyp phase, and with just a few more in the ephyra phase, and with at least 13 species of *Aurelia* (Dawson *et al.*, 2005) and possibly 350+ species in Scyphozoa (Appeltans *et al.*, 2012), there is a very low probability of distinguishing all species via polyp and/or ephyra morphology alone. Although understanding polyp and ephyra dynamics is essential to understanding blooms, equally necessary are genetics studies to link life-history stages and the morphology of medusae, which hold the greatest potential for morphologically distinguishing species of *Aurelia*.

Morphometric analyses applied to the adult medusa stage represent, with molecular analyses, a useful integrative approach to unambiguously discriminate clades. Indeed, the medusa stage may be a sufficient source of measurable morphological characters to build up a set of diagnostic characters following molecular discrimination. For example, two characters – rhopaliar and non-rhopaliar indentations – can be selected with priority to rapidly distinguish *A. coerulea* from *A. relicta* sp. nov. and *A. solida* in the Mediterranean. Some of the differentiation of *A. coerulea* from *A. relicta* sp. nov. medusae could result from differences in immaturity/maturity. Nevertheless, as most features are isometric or do not change with size, the observed result should be generally informative (although we advocate at all times possible to compare organisms of the same life-history stage).

We also note a substantial difference in the arrangement and shape of the marginal sense organ, which fits with the observations made by Browne (1905) for *A. solida*. In *A. aurita* (see Schafer, 1878; Russell, 1970), in *A. coerulea* (Nakanishi, Hartenstein & Jacobs, 2009; present study), and in *A. relicta* sp. nov. (present study) the sense organ is directed towards the bell margin, whereas in *A. solida* the sense organ is variably angled up to 90° towards the exumbrellar side (Browne, 1905; Rao, 1931). The lack of endodermal ocellus in the sense organ of *A. solida*, and the shape and arrangement of pigment granules on the ectodermal ocellus, represents another finding of distinctive character associated with rhopalium between the *Aurelia* species studied here.

Finally, we emphasize that although in some situations individual characters may differentiate some species, looking for congruence among multiple characters can better distinguish or define species. Our results, here, give support to morphometrics, as an approach that is more able to integrate the information in each character and realistically diagnose scyphozoan taxa compared with approaches applied in the past (e.g. Mayer, 1910; Kramp, 1968; Russell, 1970).

AURELIA SPP. DISTRIBUTION AND INVASION OF THE MEDITERRANEAN SEA

The Mediterranean Sea is a marine biodiversity hot spot of nearly 13 000 eukaryotic species, with a high percentage of endemism (average 20%, up to 48% in sessile taxa) and, at the same time, a crossroads of non-indigenous marine invertebrates and vertebrates, mostly of tropical (Atlantic and Indo-Pacific) origin (Bianchi & Morri, 2000; Coll *et al.*, 2010; Lejeusne *et al.*, 2010; Galil, 2012). Niche displacement, exclusion, and genetic admixture are just some of the several consequences caused by non-indigenous species to the endemic fauna (Mooney & Cleland, 2001).

Aurelia aurita, endemic to the North Atlantic and Baltic Sea, has a disjunct distribution in the Black Sea and Bosphorus Strait (Dawson & Jacobs, 2001), but so far has apparently never been identified from the Mediterranean Sea. This suggests that the ecological subtropical features of the Mediterranean Sea may not facilitate the dispersal and establishment of boreal affinity species. Furthermore, the occurrence of the three *Aurelia* species in the Mediterranean Sea is facilitated by habitat separation: (1) coastal

lagoons or marinas (Varano, Adriatic Sea; Sabaudia lake, Thyrrenian Sea; Empuriabrava, Balearic Sea) for *A. coerulea*; (2) the small marine lakes of Mljet (Croatia) for *A. relicta* sp. nov.; and (3) open-sea coastal waters for several populations of *A. solida* (Adriatic Sea, Ionian Sea, Sicily Channel, Eastern and Western Mediterranean sub-basins).

Physiological barriers may limit the homogenization of *Aurelia* species distribution and genetic admixture in the Mediterranean Sea. High phenotypic plasticity, euryvalence with respect to the main environmental factors, and life-cycle adaptations (high potential of encystment and/or asexual reproduction) may confer an ecological advantage on *A. coerulea* in enclosed habitats (Bonnet *et al.*, 2012; Marques *et al.*, 2015a), even far from its putative native geographical area (South and East China Seas). Indeed, according to Marques *et al.* (2015b), in the Thau lagoon (near Marseille) the whole life cycle of the moon jellyfish occurs entirely inside the lagoon, with no advection from and to open Mediterranean waters.

In contrast, *A. solida* is always recorded in offshore waters, suggesting an ecophysiological preference for the hydrological conditions that are typical of the Mediterranean open sea, with sea surface temperatures ranging from 12 to 27°C (Shaltout & Omstedt, 2014), representing more stable conditions than the fluctuations experienced in the semi-enclosed brackish ecosystems inhabited by congeneric *A. coerulea* (Belmonte, Scirocco & Denitto, 2011; Scorrano, 2014).

Finally, the highly confined distribution of *A. relicta* sp. nov. – exclusive to the lakes of Mljet in Croatia – might be explained by a restricted window of upper thermal tolerance. The lakes of Mljet are subject to strong seasonal water stratification, with a pronounced thermocline keeping temperatures at depths of 20–45 m constantly lower than in the surrounding Adriatic Sea at the same depth (Benović *et al.*, 2000). The persistence of *A. relicta* sp. nov. polyps throughout the year below the thermocline may therefore explain its strict endemism within the Mljet lakes.

Habitat specialists probably arose by independent adaptation to heterogeneous environments, or by different vectors and/or timing of introduction. Molecular data from previous work suggest *A. solida* (*Aurelia* sp. 8) in the Mediterranean Sea as a potential Lessepsian immigrant (Dawson *et al.*, 2005), occurring in offshore waters on both sides of the Suez Canal, as well as along the Adriatic, the Ionian Sea, and the Tunisian coasts of the Sicily Channel. In the same open sea sampling sites, no other *Aurelia* species was found.

Introductions of alien jellyfish from the Indo-Pacific province are already known. The cepheid *Marivagia stellata* Galil and Gershwin, 2010, first described from Haifa Bay (Galil *et al.*, 2010), is originally from the Indian Ocean (Galil, Kumar & Riyas, 2013). The rhizostomid *Rhopilema nomadica* Galil, 1990, now spread across the Central and Western Mediterranean (Deidun, Arrigo & Piraino, 2011; Daly Yahia *et al.*, 2013), originated from the Red Sea (Galil, Spanier & Ferguson, 1990).

As already remarked upon, the original description of *A. coerulea* is based on specimens collected in Port Jackson, one of the principle Australian harbours, at a time of a major increase in shipping trade across Pacific routes (Hewitt *et al.*, 2004). The species was later identified as *A. japonica* and *Aurelia* sp. 1 (Dawson & Jacobs, 2001; Dawson *et al.*, 2005). To date, the occurrence of *A. coerulea* in the Mediterranean Sea has only previously been suggested by DNA sequences obtained from eight specimens collected near Perpignan, in the south of France (Schroth *et al.*, 2002), a zone rich in coastal lagoons inhabited by dense populations of putative *Aurelia* sp. 1 (*A. coerulea*) and other jellyfish species, such as the non-indigenous ctenophore species *Mnemiopsis leidyi* Agassiz, 1865 (Bonnet *et al.*, 2012; Marques *et al.*, 2015a, b). Here, we identified and sampled three different populations of *A. coerulea* from coastal lagoons and harbours in different areas of the Mediterranean Sea (Balearic Sea, marina of Empuriabrava; Thyrrenian Sea, coastal lagoon of Sabaudia; Adriatic Sea, coastal lagoon of Varano). Aquaculture accounts for one of the main human activities (Cataudella & Spagnolo, 2011) in the sampled lagoons (Sabaudia, Varano), where fishermen have reported *Aurelia* jellyfish blooms following the extensive implementation of shellfish cultivation activities. The regular importing of shellfish seed could act as vectors for the introduction of *A. coerulea* polyps, which efficiently settle on bivalve shells (Miyake, Terazaki & Kakinuma, 2002; Willcox, Moltschaniwskyj & Crawford, 2008). It is noteworthy that in most Mediterranean French lagoons, oyster, clam and mussel cultivations have been intensively developed, with the Japanese oyster *Crassostrea gigas* (Thunberg, 1793) being the main crop in the area (Hoffman, 2014). Over 20 years, billions of small Japanese oysters from the North Pacific (Japan, Korea, and British Columbia) have been seeded into the Mediterranean French lagoons, together with their load of alien seaweed and invertebrate epibionts (Boudouresque *et al.*, 2011).

In addition, the site of another *A. coerulea* population, the marina of Empuriabrava (Spain), is one of the largest tourist harbours in the world, with an inner surface (near 35 km of canals) that is comparable with a coastal lagoon. Shipping and small boating (either with ballast waters or translocation of hull fouling organisms) are known to be a major

pathway for the introduction of non-native (Occhipinti-Ambrogi *et al.*, 2011) or even new species (Piraino *et al.*, 2014) into the Western Mediterranean and Adriatic Sea. Therefore, the lagoonal- or harbour-limited distribution of *A. coerulea* suggests that this species entered the Mediterranean Sea through aquaculture and/or shipping and boating vectors. Previous phylogeographic investigations demonstrated the disjunct distribution of *A. coerulea* in several localities from the Pacific coasts of Asia to California and the eastern Atlantic, evincing multiple invasions (Dawson *et al.*, 2005). According to geographic and habitat distributions, the results discussed indicate that *A. solida*, rather than *A. aurita*, is the species subject to all previous studies focusing on the Mediterranean Sea and the Adriatic Sea (e.g. Di Camillo *et al.*, 2010). An alternative perspective, that *Aurelia cruciata* Haeckel, 1880 and *Aurelia maldivensis* Bigelow, 1904 should be resurrected as valid species for the Mediterranean Sea and Red Sea (Gambill & Jarms, 2014), respectively, is difficult to assess because polyps and ephyrae provide limited taxonomic information. Both polyps and ephyrae have few morphological features, and cannot be cross-referenced to the original descriptions of medusae. Moreover, *A. maldivensis* is more distant geographically and morphologically from Mediterranean medusae than *A. solida*, and the naming of the widespread, ubiquitous, invasive *A. coerulea* is warranted by its synonymy with Kishinouye's Japanese (*A. japonica*) and von Lendenfeld's Australian type material. Further investigations on multiple localities including all life stages will be beneficial for generating convincing evidence of the affinity of *A. solida* versus *A. coerulea* within these areas.

The case of the *Aurelia* species complex investigated here provides new evidence that the Mediterranean basin is acting as a sink for non-indigenous species. The recent enlargement of the Suez Canal, one of the most potent invasion corridors in the world, is likely to increase the number of marine alien arrivals endangering the native Mediterranean biodiversity (Galil *et al.*, 2015). The risk of a long-term biotic homogenization among endemic and exotic species calls for a compelling plan of action for their management and conservation. The implementation of a broad approach, wherein integrative taxonomy represents the first step of reliable identification, would be mandatory for successfully adopting good executive practices.

ACKNOWLEDGEMENTS

We owe many thanks to colleagues for providing *Aurelia* spp. samples from several locations; in particular, we thank V. Fuentes and M. Acevedo (ICM-CSIC, Barcelona, Spain), V. Tirelli (OGS Trieste), A. Macali (CISMAR, University of Tuscia), A. Ramšak and A. Malej (Marine Biological Station, Piran, Slovenia), S.K.M. Gueroun and M.N. Daly Yahia (Faculty of Science of Bizerte), I. Onofri (University of Dubrovnik, Croatia), and C. Widmer (Point Defiance Zoo and Aquarium, Tacoma, USA). We express our gratitude to the National Park of Mljet for giving the permit for sampling in this protected area. We thank André Morandini and an anonymous reviewer for comments that improved the article. This work has received funding by the European Union projects MED-JELLYRISK (grant no. I-A/1.3/098 – ENPI CBCMED programme), VECTORS (Vectors of Change in Oceans and Seas Marine Life, Impact on Economic Sectors, grant no. 266445, FP7th programme), and CERES (Climate Change and European Aquatic Resources, grant no. 678193, Horizon 2020 programme). Logistic/technical support was also provided by the FP7 EU projects COCONET, PERSEUS, and by the Italian Flagship project RITMARE.

REFERENCES

Abramoff MD, Magalhaes PJ, Ram SJ. 2004. Image processing with ImageJ. *Biophotonics International* **11:** 36–42.

Allison DB, Paultre F, Goran MI, Poehlman ET, Heymsfield SB. 1995. Statistical considerations regarding the use of ratios to adjust data. *International journal of obesity and related metabolic disorders* **19:** 644–652.

Anderson MJ. 2001. Permutation tests for univariate or multivariate analysis of variance and regression. *Canadian Journal of Fisheries and Aquatic Science* **58:** 626–639.

Anderson MJ, Willis TJ. 2003. Canonical analysis of principal coordinates: a useful method of constrained ordination for ecology. *Ecology* **84:** 511–525.

Appeltans W, Ahyong ST, Anderson G, Angel MV, Artois T, Bailly N, Bamber R, Barber A, Bartsch I, Berta A, Blazewicz-Paszkowycz M, Bock P, Boxshall G, Boyko CB, Brandao SN, Bray RA, Bruce NL, Cairns SD, Chan TY, Cheng L, Collins AG, Cribb T, Curini-Galletti M, Dahdouh-Guebas F, Davie PJ, Dawson MN, De Clerck O, Decock W, De Grave S, De Voogd NJ, Domning DP, Emig CC, Erséus C, Eschmeyer W, Fauchald K, Fautin DG, Feist SW, Fransen CH, Furuya H, Garcia-Alvarez O, Gerken S, Gibson D, Gittenberger A, Gofas S, Gomez-Daglio L, Gordon DP, Guiry MD, Hernandez F, Hoeksema BW, Hopcroft RR, Jaume D, Kirk P, Koedam N, Koenemann S, Kolb JB, Kristensen RM, Kroh A, Lambert G, Lazarus DB, Lemaitre R, Longshaw M, Lowry J, Macpherson E, Madin LP, Mah C, Mapstone G, McLaughlin PA, Mees J, Meland K, Messing CG, Mills CE, Molodtsova TN, Mooi R, Neuhaus B, Ng PK, Nielsen C, Norenburg J, Opresko DM, Osawa M, Paulay

G, Perrin W, Pilger JF, Poore GC, Pugh P, Read GB, Reimer JD, Rius M, Rocha RM, Saiz-Salinas JI, Scarabino V, Schierwater B, Schmidt-Rhaesa A, Schnabel KE, Schotte M, Schuchert P, Schwabe E, Segers H, Self-Sullivan C, Shenkar N, Siegel V, Sterrer W, Stöhr S, Swalla B, Tasker ML, Thuesen EV, Timm T, Todaro MA, Turon X, Tyler S, Uetz P, Van der Land J, Vanhoorne B, Van Ofwegen LP, Van Soest RWM, Vanaverbeke J, Walker-Smith G, Walter TC, Warren A, Williams GC, Wilson SP, Costello MJ. 2012. The magnitude of global marine species diversity. *Current Biology* **22:** 2189–2202.

Arai MN. 1997. *A functional biology of Scyphozoa*. London: Chapman & Hall.

Bayha KM, Dawson MN. 2010. New family of allomorphic jellyfishes, Drymonematidae (Scyphozoa, Discomedusae), emphasizes evolution in the functional morphology and trophic ecology of gelatinous zooplankton. *The Biological Bulletin* **219:** 249–267.

Bayha KM, Dawson MN, Collins AG, Barbeitos MS, Haddock SH. 2010. Evolutionary relationships among scyphozoan jellyfish families based on complete taxon sampling and phylogenetic analyses of 18S and 28S ribosomal DNA. *Integrative and Comparative Biology* **50:** 436–455.

Bazinet AL, Zwickl DJ, Cummings MP. 2014. A gateway for phylogenetic analysis powered by grid computing featuring GARLI 2.0. *Systematic Biology* **63:** 812–818.

Belmonte G, Scirocco T, Denitto F. 2011. Zooplankton composition in Lake Varano (Adriatic Sea coast, Italy). *Italian Journal of Zoology* **78:** 370–378.

Benović A, Lučić D, Onofri V, Peharda M, Carić M, Jasprica N, Bobanovic-Čolić S. 2000. Ecological characteristics of the Mljet Island Sea water lakes (Southern Adriatic Sea) with special reference to their resident populations of medusae. *Scientia Marina* **64:** 197–206.

Bianchi CN, Morri C. 2000. Marine biodiversity of the Mediterranean Sea: situation, problems and prospects for future research. *Marine Pollution Bulletin* **40:** 367–376.

Boero F, Bouillon J, Gravili C, Miglietta MP, Parsons T, Piraino S. 2008. Gelatinous plankton: irregularities rule the world (sometimes). *Marine Ecology Progress Series* **356:** 299–310.

Bonnet D, Molinero JC, Schohn T, Néjib M, Yahia D, Kiel D. 2012. Seasonal changes in the population dynamics of *Aurelia aurita* in Thau lagoon. *Cahiers de Biologie Marine* **53:** 343–347.

Boudouresque CF, Klein J, Ruittons S, Verlaque M. 2011. Biological Invasion: The Thau Lagoon, a Japanese biological island in the Mediterranean Sea. In: Ceccaldi HJ, Dekeyser I, Girult M, Stora G, eds. *Global change: mankind-marine environment interactions*. Dordrecht, The Netherlands: Springer Publications, 151–156.

Brotz L, Cheung WWL, Klesiner K, Pakhomov E, Pauly D. 2012. Increasing jellyfish populations: trends in Large Marine Ecosystems. *Hydrobiologia* **690:** 3–20.

Browne ET. 1905. Scyphomedusae. *The Fauna and Geography of the Maldive and Laccadiv Archepelagos* **2**(Suppl. I)**:** 958–971.

Cataudella S, Spagnolo M. 2011. *The state of Italian marine fisheries and aquaculture*. Rome, Italy: Ministero delle Politiche Agricole, Alimentari e Forestali (MiPAAF), 620 pp.

Clarke KR, Warwick RM. 2001. *Change in marine communities: an approach to statistical analysis and interpretation*, 2nd edn. Plymouth: PRIMER-E.

Coll M, Piroddi C, Steenbeek J, Kaschner K, Ben Rais Lasram F. 2010. The biodiversity of the Mediterranean Sea: estimates, patterns and threats. *PLoS ONE* **5:** 1–36.

Daly Yahia MN, Kéfi-Daly Yahia O, Gueroun SKM, Aissi M, Deidun A, Fuentes V, Piraino S. 2013. The invasive tropical scyphozoan *Rhopilema nomadica* Galil, 1990 reaches the Tunisian coast of the Mediterranean Sea. *BioInvasions Records* **2:** 319–323.

Darriba D, Taboada GL, Doallo R, Posada D. 2012. jModelTest 2: more models, new heuristics and parallel computing. *Nature Methods* **9:** 772.

Dawson MN. 2003. Macro-morphological variation among cryptic species of the moon jellyfish, *Aurelia* (Cnidaria: Scyphozoa). *Marine Biology* **143:** 369–379.

Dawson MN. 2005. Incipient speciation of *Catostylus mosaicus* (Scyphozoa, Rhizostomeae, Catostylidae), comparative phylogeography and biogeography in south-east Australia. *Journal of Biogeography* **32:** 515–533.

Dawson MN, Hamner WM. 2009. A character-based analysis of the evolution of jellyfish blooms: adaptation and exaptation. *Hydrobiologia* **616:** 193–215.

Dawson MN, Jacobs DK. 2001. Molecular evidence for cryptic species of *Aurelia aurita* (Cnidaria, Scyphozoa). *Biological Bullettin* **200:** 92–96.

Dawson MN, Martin LE. 2001. Geographic variation and ecological adaptation in *Aurelia* (Scyphozoa, Semaeostomeae): some implications from molecular phylogenetics. *Hydrobiologia* **451:** 259–273.

Dawson MN, Raskoff KA, Jacobs DK. 1998. Field preservation of marine invertebrate tissues for DNA analyses. *Molecular Marine Biology and Biotechnology* **7:** 145–152.

Dawson MN, Gupta AS, England MH. 2005. Coupled biophysical global ocean model and molecular genetic analyses identify multiple introductions of cryptogenic species. *Proceedings of National Academy of Sciences* **102:** 11968–11973.

De Queiroz K, Gauthier J. 1992. Phylogenetic taxonomy. *Annual Review of Ecology and Systematics* **23:** 449–480.

Deidun A, Arrigo S, Piraino S. 2011. The westernmost record of *Rhopilema nomadic* (Galil, 1990) in the Mediterranean – off the Maltese Islands. *Aquatic Invasions* **6:** S99–S103.

DeSalle R, Egan MG, Siddal M. 2005. The unholy trinity: taxonomy, species delimitation and DNA barcoding. *Philosophical Transaction of the Royal Society B* **360:** 1905–1916.

Di Camillo G, Betti F, Bo M, Martinelli M, Puce S, Bavestrello G. 2010. Contribution to the understanding of seasonal cycle of *Aurelia aurita* (Cnidaria: Scyphozoa) scyphopolyps in the northern Adriatic Sea. *Journal of the*

Marine Biological Association of the United Kingdom **90:** 1105–1110.

Drummond AJ, Suchard MA, Xie D, Rambaut A. 2012. Bayesian phylogenetics with BEAUti and the BEAST 1.7. *Molecular Biology and Evolution* **29:** 1969–1973.

Felsenstein J. 1985. Confidence limits on phylogenies: an approach using the bootstrap. *Evolution* **39:** 783–791.

Folmer O, Blac M, Hoeh W, Lutz R, Vrijenhoek R. 1994. DNA primers for amplification of mitochondrial cytochrome c oxidase subunit I from diverse metazoan invertebrates. *Molecular Marine Biology and Biotechnology* **3:** 294.

Fontaine B, Van Achterberg K, Alonso-Zarazaga MA, Araujo R, Asche M, Aspöck H, Aspöck U, Audisio P, Aukema B, Bailly N, Balsamo M, Bank RA, Belfiore C, Bogdanowicz W, Boxshall G, Burckhardt D, Chylarecki P, Deharveng L, Dubois A, Enghoff H, Fochetti M, Fochetti R, Fontaine C, Gargominy O, Gomez Lopez MS, Goujet D, Harvey MS, Heller KG, van Helsdingen P, Hoch H, De Jong Y, Karsholt O, Los W, Magowski W, Massard JA, McInnes SJ, Mendes LF, Mey E, Michelsen V, Minelli A, Nieto Nafrıa JM, van Nieukerken EJ, Pape T, De Prins W, Ramos M, Ricci M, Roselaar C, Rota E, Segers H, Timm T, van Tol J, Bouchet P. 2012. New Species in the Old World: Europe as a frontier in biodiversity exploration, a test bed for 21st century taxonomy. *PLoS ONE* **7:** e36881.

Fuchs B, Wang W, Graspeuntner S, Li Y, Insua S, Herbst E, Dirksen P, Böhm A, Hemmrich G, Sommer F, Domazet T, Klostermeier UC, Anton-Erxleben F, Rosenstiel P, Bosch TCG, Khalturin K. 2014. Regulation of Polyp-to-Jellyfish transition in *Aurelia aurita*. *Current Biology* **24:** 1–11.

Galil BS. 2012. Truth and consequences: the bioinvasion of the Mediterranean Sea. *Integrative Zoology* **7:** 299–311.

Galil BS, Spanier E, Ferguson WW. 1990. The scyphomedusae of the Mediterranean coast of Israel, including two Lessepsian migrants new to the Mediterranean. *Zoologische Mededelingen (Leiden)* **64:** 95–105.

Galil BS, Gershwin LA, Douek J, Rinkevich B. 2010. *Marivagia stellata* gen. et sp. nov. (Scyphozoa: Rhizostomeae: Cepheidae), another alien jellyfish from the Mediterranean coast of Israel. *Aquatic Invasions* **5:** 331–340.

Galil BS, Kumar BA, Riyas AS. 2013. *Marivagia stellata* Galil and Gershwin, 2010 (Scyphozoa: Rhizostomeae: Cepheidae), found off the coast of Kerala, India. *BioInvasions Records* **2:** 317–318.

Galil B, Boero F, Campbell M, Carlton J, Cook E, Fraschetti S, Gollasch S, Hewitt CL, Anders J, Macpherson E, Marchini A, McKenzie C, Minchin D, Occhipinti-Ambrogi A, Ojaver H, Sergek O, Piraino S, Ruiz GM. 2015. "Double trouble": the expansion of the Suez Canal and marine bioinvasions in the Mediterranean Sea. *Biological Invasions* **17:** 973–976.

Gambill M, Jarms G. 2014. Can *Aurelia* (Cnidaria, Scyphozoa) species be differentiated by comparing their scyphistomae and ephyrae? *European Journal of Taxonomy* **107:** 1–23.

Gershwin L. 2001. Systematics and biogeography of the jellyfish *Aurelia labiata* (Cnidaria: Scyphozoa). *Biological Bullettin* **201:** 104–119.

Gershwin L, Collins AG. 2002. A preliminary phylogeny of Pelagiidae (Cnidaria, Scyphozoa), with new observations of *Chrysaora colorata* comb. nov. *Journal of Natural History* **36:** 127–148.

Gröndahl F, Hernroth L. 1987. Release and growth of *Cyanea capillata* (L.) ephyrae in the Gullmar Fjord, Western Sweden. *Journal of Experimental Marine Biology and Ecology* **106:** 91–101.

Guindon S, Gascuel O. 2003. A simple, fast and accurate method to estimate large phylogenies by maximum-likelihood. *Systematic Biology* **52:** 696–704.

Hebert PDN, Cywinska A, Ball SL, deWaard JR. 2003. Biological identifications through DNA barcodes. *Proceedings of Royal Society B* **270:** 313–321.

Heled J, Drummond AJ. 2010. Bayesian inference of species trees from multilocus data. *Molecular Biology and Evolution* **27:** 570–580.

Hérouard E. 1909. Sur les cycles évolutifs d'un Scyphistome. *Comptes Rendus de L'Académie des Sciences (Paris)* **148:** 320–323.

Hewitt CL, Campbell ML, Thresher RE, Martin RB, Boyd S, Cohen BF, Currie R, Gomon MF, Keough MJ, Lewis JA, Lockett MM, Mays N, McArthur MA, O'Hara T, Poore GCB, Ross DJ, Storey MJ, Watson JE, Wilson RS. 2004. Introduced and cryptogenic species in Port Phillip Bay, Victoria, Australia. *Marine Biology* **144:** 183–202.

Hoffman R. 2014. Alien benthic algae and seagrasses in the Mediterranean sea and their connection to global warming. In: Goffredo S, Dubinsky Z, eds. *The Mediterranean Sea*. Dordrecht, The Netherlands: Springer, 159–181.

Huang X, Madan A. 1999. CAP3: a DNA sequence assembly program. *Genome Research* **9:** 868–877.

Ki JS, Hwang DS, Shin K, Yoon WD, Lim D, Kang YS, Lee Y, Lee JS. 2008. Recent moon jelly (*Aurelia* sp. 1) blooms in Korean coastal waters suggest global expansion: examples inferred from mitochondrial COI and nuclear ITS-5.8S rDNA sequences. *ICES Journal of Marine Science* **65:** 443–452.

Kimura M. 1980. A simple method for estimating evolutionary rate of base substitutions through comparative studies of nucleotide sequences. *Journal of Molecular Evolution* **16:** 111–120.

Kishinouye K. 1891. *Aurelia japonica*, nov. sp. *Zoological Magazine (Tokyo)* **3:** 288–291.

Kramp PL. 1961. Synopsis of the medusae of the world. *Journal of the Marine Biological Association of the United Kingdom* **40:** 1–469.

Kramp PL. 1968. The scyphomedusae collected by the Galathea expedition 1950–52. *Videnskabelige Meddelelser fra den Naturhistoriske Forening i Kjöbenhavn* **131:** 67–98.

Kuniyoshi H, Okumura I, Kuroda R, Tsujita N, Arakawa K, Shoji J, Saito T, Osada H. 2012. Indomethacin induction of metamorphosis from the asexual stage to

sexual stage in the moon jellyfish, *Aurelia aurita*. *Bioscience, Biotechnology and Biochemistry* **76:** 1397–1400.

Lanfear R, Calcott B, Ho SY, Guindon S. 2012. PartitionFinder: combined selection of partitioning schemes and substitution models for phylogenetic analyses. *Molecular Biology and Evolution* **29:** 1695–1701.

Lee PLM, Dawson MN, Neill SP, Robins PE, Houghton JDR, Doyle TK, Hays GC. 2013. Identification of genetically and oceanographically distinct blooms of jellyfish. *Journal of the Royal Society Interface* **10:** 20120920.

Lejeusne C, Chevaldonné P, Pergent-Martini C, Boudouresque CF, Pérez T. 2010. Climate change effects on a miniature ocean: the highly diverse, highly impacted Mediterranean Sea. *Trends in Ecology & Evolution* **25:** 250–260.

von Lendenfeld R. 1884. The scyphomedusae of the southern hemi-sphere. Part III.—Conclusion. IV. Ordo—Discomedusae. *Proceedings of the Linnean Society of New South Wales* **9:** 259–306.

Lucas CH, Dawson MN. 2014. What are jellyfish and thaliaceans and why do they bloom? In: Pitt KA, Lucas CH, eds. *Jellyfish blooms*. Berlin: Springer, 9–44.

Maddison DR, Maddison WP. 2005. MacClade 4: analysis of phylogeny and character evolution. Version 4.08a. *The American Biology Teacher* **66:** 511–512.

Marques R, Albouy-Boyer S, Delpy F, Carré C, Le Floc'h È, Roques C, Molinero JC, Bonnet D. 2015a. Pelagic population dynamics of *Aurelia* sp. in French Mediterranean lagoons. *Journal of Plankton Research* **37:** 1019–1035.

Marques R, Cantou M, Soriano S, Molinero J-C, Bonnet D. 2015b. Mapping distribution and habitats of *Aurelia* sp. polyps in Thau lagoon, north-western Mediterranean Sea (France). *Marine Biology* **162:** 1441–1449.

Martin JW, Gershwin L, Burnett JW, Cargo DG, Bloom DA. 1997. *Chrysaora achlyos*, a remarkable new species of scyphozoan from the eastern Pacific. *Biological Bulletin* **193:** 8–13.

Mayer AG. 1910. Medusae of the world, III: the Scyphomedusae. *Carnegie Institute, Washington* **109:** 499–735.

Mishler BD, Theriot EC. 2000. The phylogenetic species concept (sensu Mishler and Theriot): monophyly, apomorphy, and phylogenetic species concepts. In: Meier R, Wheeler QD, eds. *Species concepts and phylogenetic theory*. New York, USA: Columbia University Press, 44–54.

Miyake H, Terazaki M, Kakinuma Y. 2002. On the polyps of the common jellyfish *Aurelia aurita* in Kagoshima Bay. *Journal of Oceanography* **58:** 451–459.

Mooney HA, Cleland EE. 2001. The evolutionary impact of invasive species. *Proceedings of National Academy of Sciences* **98:** 5446–5451.

Morandini AC, Marques AC. 2010. Revision of the genus *Chrysaora* Péron & Lesueur, 1810 (Cnidaria: Scyphozoa). *Zootaxa* **97:** 1–97.

Nakanishi N, Hartenstein V, Jacobs DK. 2009. Development of the rhopalial nervous system in *Aurelia* sp. 1 (Cnidaria, Scyphozoa). *Developmental Genetics and Evolution* **219:** 301–317.

Occhipinti-Ambrogi A, Marchini A, Cantone G, Castelli A, Chimenz C, Cormaci M, Froglia C, Furnari G, Gambi MC, Giaccone G, Giangrande A, Gravili C, Mastrototaro F, Mazziotti C, Orsi-Relini L, Piraino S. 2011. Alien species along the Italian coasts: an overview. *Biological Invasions* **13:** 215–237.

Ortman BD, Bucklin A, Pages F, Youngbluth M. 2010. DNA barcoding the Medusozoa using mtCOI. *Deep-Sea Research II* **57:** 2148–2156.

Padial JM, Miralles A, De la Riva I, Vences M. 2010. Review: the integrative future of taxonomy. *Frontiers in Zoology* **7:** 1–14.

Papathanassiou E, Panayotidis P, Anagnostaki K. 1987. Notes on the biology of the jellyfish *Aurelia aurita* Lam. in Elefsis Bay (SaronikosGulf, Greece). *Marine Ecology* **8:** 49–58.

Piraino S, De Vito D, Schmich J, Bouillon J, Boero F. 2004. Reverse development in Cnidaria. *Canadian Journal of Zoology* **82:** 1748–1754.

Piraino S, Aglieri G, Martell L, Mazzoldi C, Melli V, Milisenda G, Scorrano S, Boero F. 2014. *Pelagia benovici* sp. nov. (Cnidaria, Scyphozoa): a new jellyfish in the Mediterranean Sea. *Zootaxa* **3794:** 455–468.

Ramšak A, Stopar K, Malej A. 2012. Comparative phylogeography of meroplanktonic species, *Aurelia* spp. and *Rhizostoma pulmo* (Cnidaria: Scyphozoa) in European Seas. *Hydrobiologia* **690:** 69–80.

Rao HS. 1931. Notes on Scyphomedusae in the Indian Museum. *Records of the Indian Museum* **33:** 25–62.

Russell FS. 1970. *The Medusae of the British Isles. II Pelagic Scyphozoa, with a supplement to the first volume on Hydromedusae*. Cambridge: Cambridge University Press, 284 pp.

Schafer EA. 1878. Observations on the nervous system of *Aurelia aurita*. *Philosophical Transactions of the Royal Society London* **169:** 563–575.

Schroth W, Jarms G, Streit B, Schierwater B. 2002. Speciation and phylogeography in the cosmopolitan marine moon jelly, *Aurelia* sp. *BMC Evolutionary Biology* **2:** 1–10.

Scorrano S. 2014. Impacts of *Aurelia* sp. 1 outbreaks in Mediterranean coastal lagoon (Varano, SE Adriatic Coast). PhD Thesis in Ecology and Management of Biological Resources, Viterbo, Italy: Università degli Studi della Tuscia.

Shaltout M, Omstedt A. 2014. Recent sea surface temperature trends and future scenarios for the Mediterranean Sea. *Oceanologia* **56:** 411–443.

Straehler-Pohl I, Jarms G. 2010. Identification key for young ephyrae: a first step for early detection of jellyfish blooms. *Hydrobiologia* **645:** 3–21.

Straehler-Pohl I, Widmer C, Morandini AC. 2011. Characterizations of juvenile stages of some semaeostome Scyphozoa (Cnidaria), with recognition of a new family (Phacellophoridae). *Zootaxa* **2741:** 1–37.

Sukumaran J, Holder MT. 2010. DendroPy: a Python library for phylogenetic computing. *Bioinformatics* **26:** 1569–1571.

Thompson JD, Gibson TJ, Plewniak F, Jeanmougin F, Higgins DG. 1997. The CLUSTAL_X windows interface: flexible strategies for multiple sequence alignment aided by quality analysis tools. *Nucleic Acids Research* **25:** 4876–4882.

Uchida T, Nagao Z. 1963. The Metamorphosis of the Scyphomedusa, *Aurelia limbata* (Brandt). *Annotationes Zoologicae Japonenses* **36:** 83–91.

Vagelli A. 2007. New observations on the asexual reproduction of *Aurelia aurita* (Cnidaria, Scyphozoa) with comments on its life cycle on the adaptative significance. *Invertebrate Zoology* **4:** 111–127.

Vaidya G, Lohman DJ, Meier R. 2011. SequenceMatrix: concatenation software for the fast assembly of multi-gene datasets with character set and codon information. *Cladistics* **27:** 171–180.

Willcox S, Moltschaniwskyj NA, Crawford CM. 2008. Population dynamics of natural colonies of *Aurelia* sp. scyphistomae in Tasmania, Australia. *Marine Biology* **154:** 661–670.

Wrobel D, Mills C. 1998. *Pacific coast pelagic invertebrates: a guide to the common gelatinous animals*. Monterey, CA: Sea Challengers and Monterey Bay Aquarium, 108 pp.

Zwickl DJ. 2006. Genetic algorithm approaches for the phylogenetic analysis of large biological sequence datasets under the maximum likelihood criterion. PhD dissertation. Auston, TX: The University of Texas at Austin.

SUPPORTING INFORMATION

Additional supporting information may be found online in the supporting information tab for this article:

Figure S1. *COI* maximum-likelihood tree, reconstructed using GARLI 2.0.
Figure S2. *28S* maximum-likelihood tree, reconstructed using GARLI 2.0.
Table S1. Previous and new taxonomic identification, collection locality, collection ID and GenBank accession numbers of the sequences, and sample sizes.
Table S2. List of morphometric parameters in decreasing order of importance for the characterization of the morphology of *Aurelia* spp. polyps and ephyrae.
Table S3. List of morphometric parameters in decreasing order of importance for the characterization of the interspecific variation in the Mediterranean *Aurelia* spp. medusae.
Table S4. List of morphometric parameters in decreasing order of importance for the characterization of intraspecific variation of *Aurelia coerulea* medusae.